

**ÇUKUROVA UNIVERSITY
INSTITUTE OF NATURAL AND APPLIED SCIENCES**

MSc THESIS

Okan ÇELİK

**THE PROPERTIES OF NATURAL FIBER REINFORCED
HYBRID COMPOSITE MATERIALS AS AN ALTERNATIVE
TO CARBON FIBER COMPOSITES**

DEPARTMENT OF AUTOMOTIVE ENGINEERING

ADANA-2022

**ÇUKUROVA UNIVERSITY
INSTITUTE OF NATURAL AND APPLIED SCIENCES**

**THE PROPERTIES OF NATURAL FIBER REINFORCED HYBRID
COMPOSITE MATERIALS AS AN ALTERNATIVE TO CARBON FIBER
COMPOSITES**

Okan ÇELİK

MSc THESIS

DEPARTMENT OF AUTOMOTIVE ENGINEERING

We certify that the thesis titled above was reviewed and approved for the award of degree of the Master of Science by the board of jury on 06/09/2022

.....
Prof. Dr. Abdulkadir YAŞAR
SUPERVISOR

.....
Assoc. Prof. Dr. Erineç ULUDAMAR
MEMBER

.....
Assist. Prof. Dr. Şafak YILDIZHAN
MEMBER

This MSc Thesis is written at the Department of Automotive Engineering of Institute of Natural and Applied Sciences of Çukurova University.

Registration Number:

Prof. Dr. Sadık DİNÇER

Director

Institute of Natural and Applied Sciences

This MSc thesis was supported by Cukurova University Scientific Research Project Coordination (FYL-2021-13409).

Note: The usage of the presented specific declarations, tables, figures, and photographs either in this thesis or in any other reference without citation is subject to "The law of Arts and Intellectual Products" number of 5846 of Turkish Republic.

ABSTRACT

MSc THESIS

THE PROPERTIES OF NATURAL FIBER REINFORCED HYBRID COMPOSITE MATERIALS AS AN ALTERNATIVE TO CARBON FIBER COMPOSITES

Okan ÇELİK

ÇUKUROVA UNIVERSITY
INSTITUTE OF NATURAL AND APPLIED SCIENCES
DEPARTMENT OF AUTOMOTIVE ENGINEERING

Supervisor : Prof. Dr. Abdulkadir YAŞAR

Year: 2022, Pages: 95

Jury : Prof. Dr. Abdulkadir YAŞAR

: Assoc. Prof. Dr. Erineç ULUDAMAR

: Assist. Prof. Dr. Şafak YILDIZHAN

In recent years, the main goals of automotive manufacturers have been to lower production costs and minimize emissions from vehicles by reducing fuel consumption. In order to achieve these goals, it is essential to manufacture fossil fueled vehicles, and especially electric vehicles from lightweight, environmentally friendly, sustainable, and affordable materials. In this context, the importance given to hybrid composite materials is increasing in terms of their unique properties. In this study, carbon fiber reinforced polymer composites (CFRP) and hybrid composites of aramid and basalt fiber reinforced epoxy matrix were fabricated by using vacuum infusion method. Tensile test, hardness test, water absorption test, loss on ignition test, impact test, and Scanning Electron Microscopy (SEM) analysis were applied to CFRP composites and hybrid composite samples produced with different fiber ratios and arrays in order to observe the effect on mechanical properties. These tests were performed to evaluate the application of natural fiber reinforced hybrid composites as an alternative to CFRP used in the interior and exterior parts of vehicles. When the results were evaluated, it was determined that the fiber ratio and array significantly affected the mechanical properties of hybrid composites. Also, hybrid specimens had higher impact strength than CFRP composites. Through SEM analysis, fiber breakage, fiber shrinkage, fiber-matrix debonding and gaps were observed in the structure of hybrid composites.

Keywords: Hybrid composite materials, Basalt fiber, Lightweight, Vacuum infusion method, Mechanical properties

ÖZ

YÜKSEK LİSANS TEZİ

**KARBON FİBER KOMPOZİTLERE ALTERNATİF OLARAK DOĞAL
FİBER TAKVİYELİ HİBRİT KOMPOZİT MALZEMELERİN
ÖZELLİKLERİ**

Okan ÇELİK

**ÇUKUROVA ÜNİVERSİTESİ
FEN BİLİMLERİ ENSTİTÜSÜ
OTOMOTİV MÜHENDİSLİĞİ ANABİLİM DALI**

Danışman : Prof. Dr. Abdulkadir YAŞAR
Yıl: 2022, Sayfa: 95
Jüri : Prof. Dr. Abdulkadir YAŞAR
: Doç. Dr. Erinç ULUDAMAR
: Dr. Öğr. Üyesi Şafak YILDIZHAN

Son yıllarda, otomotiv üreticilerinin ana hedefleri üretim maliyetlerini düşürmek ve yakıt tüketimini azaltarak araçlardan yayılan emisyonları en aza indirmek olmuştur. Bu hedeflere ulaşabilmek için, fosil yakıtlı araçların ve elektrikli araçların hafif, çevre dostu, sürdürülebilir ve uygun fiyatlı malzemelerden üretilmesi gerekmektedir. Bu bağlamda, hibrit kompozit malzemelere verilen önem benzersiz özellikleri bakımından artmaktadır. Bu çalışmada, karbon fiber takviyeli polimer kompozitler (CFRP) ile aramid ve bazalt elyaf takviyeli epoksi matrisli hibrit kompozitler vakum infüzyon yöntemi kullanılarak üretilmiştir. CFRP kompozitlerine ve mekanik özelliklere etkisini gözlemlemek amacıyla farklı elyaf oranı ve dizilimleriyle üretilen hibrit kompozit malzemelere çekme testi, sertlik testi, su emdirme testi, yanma kaybı testi, darbe testi ve taramalı elektron mikroskopu (SEM) analizi uygulanmıştır. Bu testler, doğal elyaf takviyeli kompozitlerin araçların iç ve dış kısımlarında kullanılan CFRP kompozitlerine alternatif olarak uygulanmasını değerlendirmek amacıyla gerçekleştirilmiştir. Sonuçlar değerlendirildiğinde, fiber oranı ve diziliminin hibrit kompozitlerin mekanik özelliklerini önemli ölçüde etkilediği belirlenmiştir. Ayrıca, hibrit numunelerin CFRP kompozitlerinden daha yüksek darbe dayanımına sahip olduğu saptanmıştır. SEM analizi ile hibrit kompozitlerin yapısında fiber kırılması, fiber büzülmesi, fiber-matris bağ kopması ve boşluklar olduğu gözlemlenmiştir.

Anahtar Kelimeler: Hibrit kompozit malzemeler, Bazalt fiber, Hafif, Vakum infüzyon yöntemi, Mekanik özellikler

GENİŞLETİLMİŞ ÖZET

İnsanlar, ilk çağlardan bu yana sayısız türde malzeme üretmiş ve kullanmıştır. Yıllar boyunca, insanların ihtiyaçları yaşam koşullarına göre değişiklik göstermiş; ihtiyaçlarını karşılamak için girdikleri arayışlar sonucunda yeni türde malzemeler keşfetmişler ve geliştirmişlerdir. İnsanların yerleşik hayata geçmesi ve hızla artan insan nüfusu, malzeme gereksiniminin de hızla artmasına neden olmuştur. Bu durum, malzeme talebinin karşılanabilmesi için teknolojinin de zaman içinde gelişmesiyle birçok endüstri kolunda sanayinin kurulmasına ve seri üretime geçilmesine öncülük etmiştir.

Son yıllarda, bu endüstrilerde artan rekabet nedeniyle yüksek performanslı, korozyona ve aşınmaya karşı dayanıklı, çevreye daha az zarar veren, hafif ve mukavemeti yüksek malzemeler elde etmek üreticilerin ana hedefi olmuştur. Kompozit malzemeler, malzeme bilimi alanında yapılan geniş kapsamlı çalışmalar ve gelişen teknoloji sayesinde denizcilik, savunma sanayi, inşaat, uzay ve havacılık, raylı sistemler, spor ekipmanları, otomotiv gibi birçok alanda kullanılmaya başlanmış ve üreticilerin amaçlarını gerçekleştirmesine olanak sağlamıştır.

Kompozitler, iki ya da daha fazla farklı malzemenin, birbirleri içinde çözünmeden çeşitli üretim teknikleriyle bir araya getirilerek, bileşenlerden herhangi birinde olmayan özelliklerin ortak bir yerde toplanmasıyla elde edilen, üstün özellikli malzemelerdir. Kompozit malzeme üretiminde ana hedef çekme dayanımı, yorulma dayanımı, korozyon ve aşınma direnci, akustik iletkenlik, kırılma tokluğu, ısı ve elektriksel direnç, yalıtım, ağırlık, görünüm gibi özelliklerden bir veya birkaçını geliştirilmiştir. Kompozitler genellikle bir matris malzemesinden ve takviye elemanı adı verilen bir malzemedен oluşmaktadır. Ayrıca özelliklerin iyileştirilebilmesi için kompozit malzemelere dolgu veya katkı maddeleri de eklenebilmektedir. Kompozitler, genellikle matris malzemesi, takviye elemanı veya takviye tipine göre sınıflandırılırlar. Bu çalışmanın konusu olan hibrit

kompozit malzemeler ise, iki veya daha fazla farklı tipteki fiberin bir araya getirilmesiyle oluşan malzemelerdir. Hibrit kompozitlerde amaç, farklı tipteki fiberleri tek bir matris içerisinde bir araya getirerek mekanik özellikleri zayıf olan fiberin dezavantajını diğer bir fiber takviyesiyle gidermektir.

Sanayinin gelişmesi ve seri üretime geçilmesiyle birçok sektörde metal malzemelerden yararlanılmıştır. Ancak, son yıllarda yapılan araştırmalar kompozit malzemelerin metallere karşı iyi bir alternatif olduğunu göstermiş ve farklı alanlarda kullanımı hızla artmaya başlamıştır. Günümüzde, birçok mühendislik alanında kompozit malzemeler tercih edilmekte ve uygulama alanları günden güne genişlemektedir.

Günümüzde, birçok sektörde üretim maliyetleri ve sürdürülebilirlik gibi konularda hassasiyet artmaktadır. Otomotiv endüstrisinde de bu konulara ek olarak araçların yaydığı emisyonlar ve bu emisyonların neden olduğu çevre kirliliği ve küresel ısınma gibi sorunlar endişe verici boyutlara ulaşmıştır. Bu durumun önüne geçebilmek için, birçok devlet tarafından radikal düzenlemeler yürürlüğe konulmuştur. Bu düzenlemeler, başta otomotiv olmak üzere birçok endüstri kolunda kullanılmakta olan mevcut malzemelerin değişmesine ve yeni malzemelerin geliştirilerek kullanılmasına yol açmıştır.

Bu doğrultuda yapılan çalışmalar, malzeme seçimi için elyaf takviyeli kompozit malzemelerin en uygun potansiyele sahip alan olduğunu göstermektedir. Elyaf takviyeli polimer matris kompozitler, çelik gibi yaygın metal malzemelerden daha büyük miktarlarda, daha dayanıklı ve daha hafif olarak üretilebilmeleri sayesinde otomotiv endüstrisi de dahil olmak üzere birçok sektörde tercih edilmektedir.

Kompozitlerde takviye elemanı olarak kullanılan elyaflar, doğal ve sentetik elyaf olmak üzere iki gruba ayrılırlar. Sentetik elyaflardan karbon fiber, aramid fiber (kevlar) ve cam fiber kompozit üretiminde en yaygın kullanılan malzemelerdendir. Doğal elyaflarda ise jüt ve keten sık kullanılan malzemeler arasında olmakla birlikte, son zamanlarda bazalt elyafı mekanik özelliklerinden

dolayı popülerlik kazanmıştır. Doğal fiber takviyeli kompozitler, düşük mukavemet ve düşük sertlik gibi bazı dezavantajlara sahip olduklarından dolayı takviye elemanı olarak yapısal uygulamalarda ilk sırada tercih edilmemektedirler. Ancak, düşük yoğunluk, esneklik ve tokluk gibi özelliklerinin yanı sıra bulunabilirlik, sağlık riskinin daha az olması ve düşük maliyet gibi özelliklere de sahip olduklarından dolayı doğal fiberlere olan ilgi mühendislik çalışmalarında giderek artmaktadır.

Bu alanda yapılan çalışmalar sonucunda, hibridizasyon yöntemi ile aynı matriste birden fazla elyaf türü bir araya getirilerek doğal ve sentetik elyafların zayıf yönleri mümkün olduğunca ortadan kaldırılmış ve darbe enerjisini absorbe etme kabiliyeti yüksek, daha hafif, nispeten çevre dostu ve sürdürülebilir malzemeler ortaya çıkmıştır. Bu sayede otomotiv üreticileri, araçların ağırlığını düşürerek çevreye yayılan emisyonları azaltmak için yüksek mukavemet / düşük ağırlık oranına sahip bu tür malzemelerin kullanımına yönelmişlerdir.

Bu çalışmada, sentetik ve doğal elyaflardan yeni nesil bir hibrit kompozit malzeme üretilmiş; araçların iç ve dış kısımlarında kullanılan karbon fiber kompozitlerine alternatif, daha hafif ve daha düşük maliyetli bir malzeme olarak geliştirilip kullanılması amaçlanmıştır. Bunun yanı sıra, dayanıklılığın çok önemli bir rol oynadığı askeri alanda zırhlı araçların üretiminde kullanılması bakımından mekanik özellikleri araştırılmıştır. Bu doğrultuda, aramid elyafının bazalt elyafı ile oluşturacağı hibrit yapılar incelenip analiz edilmiş, hibrit kompozitler ile karbon fiber kompozitlerinin mekanik özellikleri karşılaştırılmıştır.

Bu çalışmada, 170 g/m² ağırlığında olan aramid elyafı ile 210 g/m² ağırlığında olan bazalt elyafından yirmi farklı hibrit kompozit örneği ve 245 g/m² ağırlığa sahip karbon elyafından beş farklı karbon fiber takviyeli polimer (CFRP) kompozit örneği elde edilmiştir. Matris elemanı olarak epoksi reçine tercih edilirken, kompozit malzemelerin üretiminde vakum infüzyon (ayrıca vakum destekli reçine transfer kalıplama olarak da adlandırılır) yöntemi kullanılmıştır.

Tüm kompozit örnekleri, uygulanacak test standartlarına uygun olması açısından farklı testler için standartlarda belirtilen boyutlarda üretilmiştir. Ayrıca, hibrit yapıların içeriğindeki fiberlerin katman sayısı ve dizilimleri, malzemelerin mekanik özelliklerine olan etkisini gözlemek amacıyla değiştirilerek üretilmiştir. Üretilen kompozit yapılara mekanik özelliklerini belirlemek için Charpy çentik darbe testi, çekme testi ve Rockwell sertlik testi uygulanmış; belirli bir süre su dolu kaplarda bekletilerek su emilim testi, elektrikli kül fırınında yanma kaybı testi gerçekleştirilmiş ve SEM analizi ile numunelerin morfolojik yapısı incelenmiştir. Üretilen hibrit kompozit numunelerin araçların dış kısımlarının yanı sıra iç mekânda da kullanımı incelendiğinden, mekanik test dışındaki su emilimi analizinin üretilen malzemeler için gerekli olduğu sonucuna varılmıştır. Bu analizler, otomobillerin kullanıldıkları sürede iç mekândaki nem artışının malzemenin yapısını nasıl etkilediğini gözlemek için yapılmıştır.

Charpy çentik darbe testi sonucunda, eşit oranda aramid ve bazalt elyafı içeren hibrit kompozitlerin en yüksek darbe enerjisine, karbon fiber kompozitlerinin ise gevrek yapısından dolayı en düşük darbe enerjisi emilim kapasitesine sahip olduğu tespit edilmiştir. Ayrıca, aramid elyafın bileşim oranındaki azalma sonucunda hibrit kompozitlerin darbe enerjisinde yaklaşık 35% düşüş olduğu gözlemlenmiştir. Yanma kaybı testi sonuçları incelendiğinde, kompozit numunelerin birbirine çok yakın oranda ağırlık kaybettiği görülmüştür. Karbon fiber numunelerin ağırlıklarının ortalama 1,69%'unu, B4A3 dizilimindeki hibrit kompozitlerin ise ağırlıklarının 2,06%'sını kaybettiği belirlenmiştir. Su emilim testi sonucunda, karbon fiber kompozitleri 0,34% ile en az su emme kapasitesine sahip malzemeler olurken, hibrit kompozitlerdeki bazalt elyafı oranının artmasıyla malzemelerin su emme kapasitelerinin de arttığı görülmüştür. Çekme testi sonuçlarına bakıldığında, CFRP kompozitlerinin ortalama gerilme mukavemetinin 852 MPa, buna en yakın değer olan B6A6 dizilimindeki hibrit kompozitlerin ortalama gerilme mukavemetinin ise 572 MPa olduğu saptanmıştır. B6A6 numuneleri ile aynı oranda bazalt ve aramid elyafı içermesine rağmen farklı

fiber dizilimine sahip A6B6 numunelerinin yaklaşık 17% daha düşük gerilme mukavemetine sahip olduğu görülmüştür. Çekme testinin ve Charpy çentik darbe testinin sonuçlarını daha iyi analiz edebilmek için, SEM ile test sonrası kırılan kompozit numunelerin morfolojik yapısı incelenmiştir. SEM görüntülerinden, karbon fiber ile epoksi matrisinin güçlü bir bağ kurduğu ve malzeme yapısında boşluk olmadığı tespit edilirken, hibrit kompozitlerde CFRP kompozitlerine kıyasla fiber kırılması, delaminasyon, fiber-matris ayrılması ve boşluklu yapının olduğu görülmüştür. Sertlik testi sonuçları incelendiğinde, karbon fiber kompozitinin 61,7 HRC ile en yüksek değere sahip olduğu görülürken, bu değeri 55,7 HRC ile A24B24 sıralamasına sahip ve 50,4 HRC ile A17B32 diziliminde olan hibrit kompozit malzemelerin takip ettiği tespit edilmiştir.



ACKNOWLEDGEMENTS

First of all, I would like to express my sincere gratitude to my supervisor, Prof. Dr. Abdulkadir YAŞAR, for his support, motivation and encouragement throughout preparation of this thesis.

Besides my advisor Prof. Dr. Abdulkadir YAŞAR, I sincerely thank Res. Assist. Berkay KARAÇOR and Res. Assist. Himmət ÖZARSLAN for sharing their knowledge and valuable time for this work.

I would like to thank to all Automotive Engineering Department academic personals Prof. Dr. Kadir AYDIN, Prof. Dr. Ali KESKİN, Prof. Dr. Mustafa ÖZCANLI, Assoc. Prof. Dr. Hasan SERİN, and Assoc. Prof. Dr. M. Atakan AKAR, Assist. Prof. Dr. Tayfun ÖZGÜR, Assist. Prof. Dr. Erdi TOSUN, and Assist. Prof. Dr. Şafak YILDIZHAN.

Last but not least, I sincerely thank my parents. I would not have succeeded in my thesis without their support and motivation.

I also thank Cukurova University Scientific Research Project Coordination (Project ID: FYL-2021-13409) for financial support to this project.

CONTENTS	PAGE
ABSTRACT.....	I
ÖZ	II
GENİŞLETİLMİŞ ÖZET	III
ACKNOWLEDGEMENTS	IX
CONTENTS.....	X
LIST OF TABLES	XII
LIST OF FIGURES	XIV
LIST OF ABBREVIATIONS AND NOMENCLATURE	XVIII
1. INTRODUCTION	1
2. PRELIMINARY WORK.....	9
2.1. Composites	9
2.2. Hybrid Composites	10
2.3. Polymer Matrix Composites	16
2.3.1. Matrix Material	16
2.3.1.1. Thermosets	17
2.3.1.2. Thermoplastics	17
2.4. Reinforcement.....	18
2.5. Manufacturing Methods of Composites.....	19
2.5.1. Hand Lay-up	21
2.5.2. Filament Winding.....	21
2.5.3. Vacuum Bagging.....	22
2.5.4. Pultrusion	23
2.5.5. Resin Transfer Molding	24
2.5.6. Vacuum Infusion.....	25
3. MATERIAL AND METHOD	27
3.1. Materials	27
3.1.1. Carbon Fiber	27

3.1.2. Aramid Fiber (Kevlar).....	27
3.1.3. Basalt Fiber	28
3.1.4. Matrix Materials.....	31
3.2. Method.....	32
3.2.1. Preparation Process of Matrix Materials.....	32
3.2.2. Manufacturing of Composite Materials	32
3.2.3. Experimental	41
3.2.3.1. Tensile Test Analysis	41
3.2.3.2. Impact Test Analysis	44
3.2.3.3. Morphological Analysis	50
3.2.3.4. Loss on Ignition Test Analysis	51
3.2.3.5. Water Absorption Analysis	53
3.2.3.6. Hardness Test Analysis	54
4. RESULTS AND DISCUSSIONS.....	57
4.1. Tensile Test Analysis Results	57
4.2. Impact Test Analysis Results.....	64
4.3. Morphological Analysis Results.....	67
4.4. Loss on Ignition Test Analysis Results.....	77
4.5. Water Absorption Analysis Results.....	78
4.6. Hardness Test Analysis Results	81
5. CONCLUSIONS.....	83
REFERENCES	87
CURRICULUM VITAE.....	95

LIST OF TABLES	PAGE
Table 1.1. Natural fibers in automotive components.....	5
Table 2.1. Fabricated composite plates from top surface to bottom surface	15
Table 3.1. Properties of Basalt fiber and synthetic fibers.....	29
Table 3.2. Properties of fabrics.....	30
Table 3.3. Epoxy and hardener properties.....	32
Table 3.4. Composite codes and composite contents of produced materials	34
Table 3.5. Composite codes and fiber layouts for Tensile test.....	35
Table 3.6. Composite codes and fiber layouts for Charpy Impact test and Rockwell Hardness test	35
Table 3.7. Composite codes and fiber layouts for Water Absorption test.....	36
Table 3.8. Composite codes and fiber layouts for Loss on Ignition test	36
Table 3.9. Specification of Charpy Impact Testing Machine.....	47
Table 4.1. Tensile test results	61
Table 4.2. Ignition loss test results of composite samples.....	77



LIST OF FIGURES	PAGE
Figure 1.1. Electric vehicle production by automobile manufacturer	2
Figure 1.2. Historical shift in vehicle composition by mass	3
Figure 2.1. Categorization of composite materials.....	9
Figure 2.2. Types of natural fibers classified by source of their origin.....	19
Figure 2.3. Composite processing techniques.....	20
Figure 2.4. Typical hand lay-up process	21
Figure 2.5. Schematic of filament winding process	22
Figure 2.6. Schematic of vacuum bagging process	23
Figure 2.7. Pultrusion process.....	23
Figure 2.8. RTM process.....	24
Figure 2.9. Typical vacuum infusion method.....	25
Figure 3.1. Price comparison of Basalt fiber and synthetic fibers.....	30
Figure 3.2. Fabric samples respectively; a) Carbon fiber (245 g/m ²), b) Aramid fiber (170 g/m ²), c) Basalt fiber (210 g/m ²).....	31
Figure 3.3. The cleaned surface area determined by vacuum sealing tape	38
Figure 3.4. Mold release wax applied to the surface.....	38
Figure 3.5. Vacuum hoses attached to system and layered fabrics were placed in frame.....	39
Figure 3.6. Peel ply laid on the sample	39
Figure 3.7. Infusion mesh laid on the sample.....	40
Figure 3.8. Vacuum bag attached to system and air inside the system vacuumed.....	40
Figure 3.9. Fully resin impregnated material	41
Figure 3.10. Dimensions of the tensile test specimen according to ASTM D 3039 standard.....	42
Figure 3.11. Tensile test specimens; a) A4B8, b) B8A4, c) B6A6, d) A6B6, e) C9.....	43

Figure 3.12.	Tensile testing machine	44
Figure 3.13.	Dimensions of Charpy type test specimen.....	45
Figure 3.14.	Composite material samples which produced for Charpy impact test; a) A17B32, b) B24A24, c) A24B24, d) B32A17, e) C44.....	46
Figure 3.15.	Notching device	47
Figure 3.16.	Impact testing unit	48
Figure 3.17.	Sample placed to test region	49
Figure 3.18.	Data screen of Charpy impact test machine.....	50
Figure 3.19.	Scanning electron microscope	51
Figure 3.20.	Electric muffle furnace	52
Figure 3.21.	Water absorption of test samples; a) B5A4, b) B6A3, c) A3B6, d) C9, e) A5B4	54
Figure 3.22.	Hardness test machine	55
Figure 4.1.	Stress-Strain graph of a C9 composite material.....	57
Figure 4.2.	Stress-Strain graph of a B6A6 hybrid composite material	58
Figure 4.3.	Stress-Strain graph of a A6B6 hybrid composite material	58
Figure 4.4.	Stress-Strain graph of a B8A4 hybrid composite material	59
Figure 4.5.	Stress-Strain graph of a A4B8 hybrid composite material	59
Figure 4.6.	Samples after Tensile test, left to right; C9, A6B6, B6A6, A4B8, B8A4	60
Figure 4.7.	Average tensile strength of composite materials	62
Figure 4.8.	Average elongation rate of composite materials.....	63
Figure 4.9.	Average elastic modulus of composite materials.....	64
Figure 4.10.	Impact energy values of produced composite samples.....	65
Figure 4.11.	Impact strength of composite samples produced	66
Figure 4.12.	Samples after Charpy impact test, from left to right; C44, B24A24, A24B24, B32A17, A17B32	66
Figure 4.13.	SEM image of C9 sample after tensile test (X100)	68

Figure 4.14.	SEM image of C9 sample after tensile test (X500)	68
Figure 4.15.	SEM image of B8A4 sample after tensile test (X100).....	69
Figure 4.16.	SEM image of B8A4 sample after tensile test (X500).....	69
Figure 4.17.	SEM image of A4B8 sample after tensile test (X100).....	71
Figure 4.18.	SEM image of A4B8 sample after tensile test (X500).....	71
Figure 4.19.	SEM image of B6A6 sample after tensile test (X100).....	72
Figure 4.20.	SEM image of B6A6 sample after tensile test (X500).....	72
Figure 4.21.	SEM image of A6B6 sample after tensile test (X100).....	73
Figure 4.22.	SEM image of A6B6 sample after tensile test (X500).....	73
Figure 4.23.	SEM image of C44 sample after impact test (X250)	74
Figure 4.24.	SEM image of B32A17 sample after impact test (X250)	75
Figure 4.25.	SEM image of A17B32 sample after impact test (X250)	75
Figure 4.26.	SEM image of B24A24 sample after impact test (X250)	76
Figure 4.27.	SEM image of A24B24 sample after impact test (X250)	76
Figure 4.28.	Water absorption of C9 composite material	78
Figure 4.29.	Water absorption of A3B6 hybrid material	79
Figure 4.30.	Water absorption of B4A5 hybrid material	79
Figure 4.31.	Water absorption of B6A3 hybrid material	80
Figure 4.32.	Water absorption of A5B4 hybrid material	80
Figure 4.33.	Hardness values of composite materials	82



LIST OF ABBREVIATIONS AND NOMENCLATURE

GHGs	:	Greenhouse gases
CO ₂	:	Carbon Dioxide
IPCC	:	Intergovernmental Panel on Climate Change
C	:	Celsius
IEA	:	International Energy Agency
EV	:	Electric vehicle
ICE	:	Internal combustion engine
%	:	Percentage
GFRP	:	Glass fiber reinforced polymer
CFRP	:	Carbon fiber reinforced polymer
NFRCs	:	Natural fiber reinforced composites
J	:	Joule
SEM	:	Scanning Electron Microscopy
i.e.	:	Id est
BFRP	:	Basalt fiber reinforced polymer
FRP	:	Fiber reinforced polymer
AFRP	:	Aramid fiber reinforced polymer
g/m ²	:	Gram per square meter
LVI	:	Low-velocity impact
PP	:	Polypropylene
etc.	:	Et cetera
NIJ	:	National Institute of Justice
ISO	:	International Organization for Standardization
PMCs	:	Polymer-matrix composites
PEEK	:	Polyetheretherketone

PPS	:	Polyphenylene sulfur
PEI	:	Polyetherimide
PMMA	:	Polymethyl methacrylate
e.g.	:	Exempli gratia
PET	:	Polyethylene terephthalate
PBT	:	Polybutylene terephthalate
g/cm ³	:	Gram per cubic centimeter
mm	:	Millimeter
µm	:	Micrometer
USD	:	United States Dollar
\$/kg	:	Dollars per kilogram
\$/m ²	:	Dollars per square meter
MPa	:	Megapascal
GPa	:	Gigapascal
UV	:	Ultraviolet
KF	:	Kenaf fiber
USA	:	United States of America
PPTA	:	Poly-para-phenylene-terephthalamide
GRP	:	Glass-reinforced plastic
PA	:	Polyamide
RTM	:	Resin transfer molding
VARTM	:	Vacuum-assisted resin transfer molding
mPas	:	Millipascal second
mg	:	Milligram
KOH	:	Potassium hydroxide
ASTM	:	American Society for Testing and Materials
mm/min	:	Millimeter per minute
kN	:	Kilonewton

V : Volt
kV : Kilovolt
g : Gram
kgf : Kilogram force
N/mm² : Newton per square millimeter
kJ/mm : Kilojoule per millimeter
CUMERLAB : Cukurova University Central Research
Laboratory
HRC : Rockwell Hardness Value



1. INTRODUCTION

The transportation needs of people increased significantly due to the enormous increase in the world population in the last century. This situation resulted in higher demand for vehicles, and therefore the automotive industry has become one of the most important sectors in many countries. However, the increasing number of fossil-fueled vehicles has increased emissions of greenhouse gases (GHGs) and damaged the environment by causing global warming and climate change. In addition to that, rising fuel prices and vehicle production costs have pushed automotive manufacturers to find novel solutions in order to minimize or eliminate these issues.

The increasing emissions - especially carbon dioxide (CO₂) - continue to affect the environment severely due to rising global vehicle ownership. In order to observe these effects, multiple scientific research was conducted. As a consequence, it was forecasted by Intergovernmental Panel on Climate Change (IPCC) that the earth's temperature will rise 1° to 2° Celsius (C) by 2020, and 2° to 5°C by 2070 because of emissions from vehicles (OECD, 2002). It was also predicted by International Energy Agency (IEA) that the average temperature of the earth will rise 6°C by 2100 unless some measures are taken to reduce GHG emissions (Kongwat et al., 2021).

Owing to increasing environmental concerns and government regulations about the reduction of CO₂ emissions, various vehicle technologies such as regenerative braking systems, engines with higher fuel efficiency, lesser drag losses, and lightweight design are considered by automotive manufacturers (Ji, 2015). In addition, electric vehicle (EV) production and ownership are ramping up day by day since EVs have zero exhaust emission, while the vehicles with internal combustion engine (ICE) are being manufactured less by the automotive companies to eliminate emissions as much as possible. Electric vehicle production and sales numbers year by year are shown in Figure 1.1.

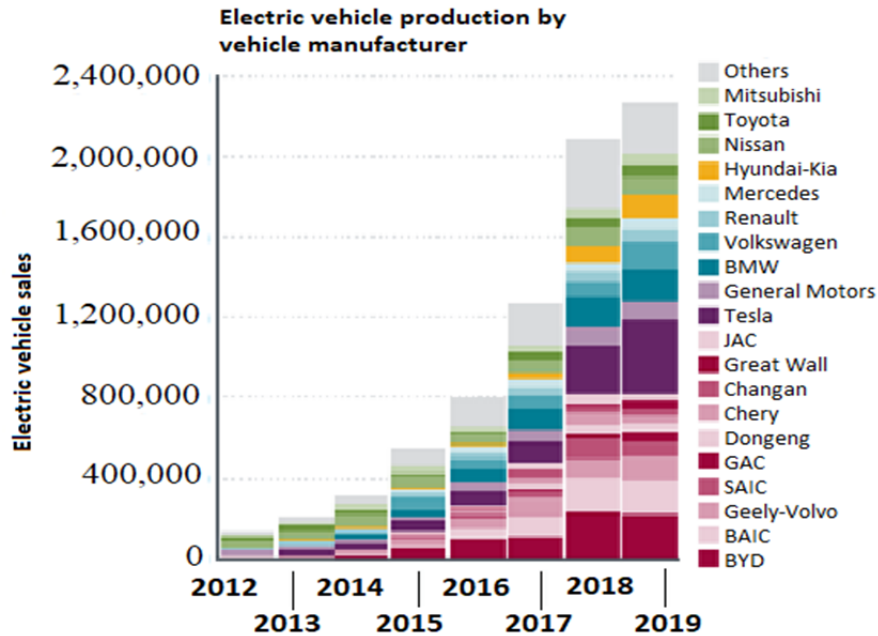


Figure 1.1. Electric vehicle production by automobile manufacturer (based on EV Volumes, 2020)

In recent years, automotive manufacturers have begun to focus on the lightweight design in vehicles in order to get higher fuel efficiency and lower vehicle emissions as a result. In this way, the lesser vehicle emissions contribute to reduce greenhouse effects. Besides, the reduction of fuel consumption reduces the dependency on limited fuel resources. The calculations indicated that nearly 250 million barrels of crude oil can be saved by a 25% reduction in vehicle weight (Safri et al., 2018). Thus, the increasing fuel prices could also be prevented by less demand of fossil fuels.

In addition, the travel range of a typical EV without a recharge is unsatisfactory owing to limited energy storage. So, lightweight design has become crucially important to reduce energy consumption alongside the battery capacity since weight is one of the main factors limiting the travel distance. Therefore, the longer distances can be traveled by lighter vehicles and material technology is one of the most effective approaches making vehicles lighter (Liu et al., 2013).

In the automotive industry, most of the parts in vehicles are made of conventional metals such as steel, aluminum, magnesium and so on. Lately, automotive manufacturers have begun to substitute these materials with composites to be able to produce much lighter parts. Composite materials have many advantages such as lightweight, higher strength to weight ratio, higher fatigue and corrosion resistance, and easy formability in comparison to conventional metals. On the other hand, composites also have some downsides such as high manufacturing cost, high cost of raw materials, various production methods from the conventional techniques and difficulty of mass production (Ji, 2015).

Composite materials are widely used in civil engineering, aerospace industry, sports equipment, marine industry, military applications etc., as in the automotive industry. The usage of composites in the automotive industry has considerably increased in decades due to the advantages they provide, as mentioned before. In history, Chevrolet Corvette was the first car whose body made from glass fiber reinforced polymer (GFRP) composites in 1953 (Mangino et al., 2007). Figure 1.2 illustrates the increase of composite materials used in vehicle production over a century and the expected vehicle material content in the future.

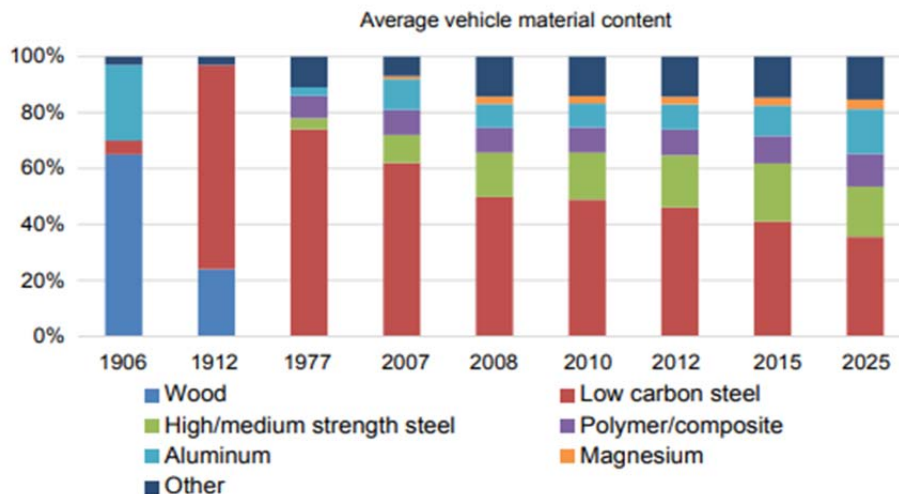


Figure 1.2. Historical shift in vehicle composition by mass (Mayyas et al., 2016)

Recently, composite material usage in production of vehicle parts such as bumpers, door panels, dashboard, leaf springs, body panels, has been increasing regularly and it is expected this increase to last in the future. Especially carbon fiber reinforced polymer (CFRP) composites are often used in lightweight design applications in vehicles to reduce fuel and energy consumption by reducing the vehicle weight. According to research work, if structural parts were designed properly, a weight reduction of 50% could be obtained by using CFRP instead of steel in vehicle components. Various applications could be seen in different vehicles such as luxury cars, Formula 1 cars and so on. For instance, in BMW i3, which is an electric vehicle, most of the internal parts and body structure were made of CFRP composites. Thus, a weight reduction of 30% was obtained in this application (Ji, 2015). However, the high cost of carbon fiber makes widespread usage of CFRP composites incredibly difficult as a structural component in automotive applications. Furthermore, carbon fiber is neither environmentally friendly nor bio-renewable material due to being synthetic fiber.

Sustainability and increasing environmental concerns have led researchers to develop effective and new materials by taking advantage of natural sources. After comprehensive research, natural fibers have gained lots of attention due to not only having low cost and lightweight but also being eco-friendly, bio-renewable, biodegradable and easily available. Natural fibers could be derived from plants, minerals, and animals. Natural fiber reinforced composites (NFRCs), especially plant-based ones due to being more cost effective, have been increasingly used in different vehicle exterior and interior parts such as vehicle bonnet, head liners, package trays, door panels, dashboards, and seat backs (Naik et al., 2022). Various NFRCs used in vehicle components by different automotive manufacturers are introduced in Table 1.1.

Table 1.1. Natural fibers in automotive components (Chauhan et al., 2019)

Manufacturers	Model	Applications	Natural Fiber
Daimler Chrysler	A, C, E, and S Class	Door and floor panels, trunk panels, dashboards, pillar cover panels, seat back rests, insulation	Flax, sisal, coir, wood, banana, cotton
BMW	3, 5, and 7 series	Door panels, boot linings, seat backs, headliner panels, noise insulation panels	Flax, sisal, cotton, wood, hemp
Audi	A2, A3, A4, A6, A8, A4 Avant, Coupe, Roadster	Seat backs, back and side door panels, boot liners, spare tire liners	Flax, sisal
Volkswagen	Golf, Passat, Bora	Seat backs, door panels, boot liners, boot lid finish panels	Flax, sisal
Ford	Mondeo, Focus	Door panels, boot liners, floor trays, door inserts	Kenaf, wheat, castor
Toyota	Raum, Brevis, Harrier, Celsior	Floor mats, spare tire covers, door panels, seat backs, luggage compartments	Kenaf, sugarcane, bamboo
General Motors	Cadillac DeVille, Chevy Traiblazer, Chevy Impala, GMC Envoy	Seat backs, cargo area floor mats, noise insulation, door panels, trim	Cotton, flax, wood, kenaf, hemp
Opel	Vectra, Astra, Zafira	Door panels, head liner panels, instrumental panels	Flax, kenaf
Lotus	Eco Elsie	Body panels, interior mats, seats	Hemp, sisal
Peugeot	406	Front and rear door panels, seat backs, packaging trays	
Fiat	Punto, Brava, Alfa Romeo 146, 156, 159	Door panels	
Volvo	V70, C70	Seat cushions, cargo floor mats	
Mitsubishi		Cargo area floors, door panels, instrument panels	

Despite all the advantages such as being non-toxic, renewable, and cost-effective, natural fibers also have many disadvantages that must be considered. The mechanical properties of natural fibers depend on the geographical and environmental conditions such as rain, sun, the soil in which the plant is grown, harvesting season and which part of the plant harvested (Koronis et al., 2013). Furthermore, natural fibers have low impact strength, poor fire and moisture resistance.

Composites are steadily becoming more attractive day by day as a material choice in different industrial applications due to their high strength-to-weight ratios. However, the mechanical properties of natural fibers are usually lower than synthetic counterparts. The low mechanical properties are an obstacle developing high performance materials for structural applications. Comprehensive studies have demonstrated that the hybridization of natural and synthetic fibers is an effective way to increase their mechanical performance. Hybrid composites have superior mechanical properties since the disadvantages of one type of fiber could be overcome by the advantages of the other type of fiber. As a result, optimal performance in terms of mechanical properties, cost-effectiveness and sustainability could be achieved by proper hybrid composite material design (Flynn et al., 2016).

The purpose of this research thesis is to investigate the usability of hybrid composite materials made of natural and synthetic fibers as an alternative to carbon fiber reinforced polymer composites used in vehicle components and additionally in production of armored military vehicles. In hybrid composite samples manufactured with this study, basalt fiber and aramid fiber were preferred as reinforcement materials. As the matrix material, epoxy resin was used both in hybrid composites and pure carbon fiber composites. All the composite products were manufactured by vacuum infusion method. The usability of these hybrid composites instead of carbon fiber composites in the automotive industry was examined by analyzing not only the mechanical and thermal properties but also

microscopic structure of these composite specimens. Hence, the usage of materials which are environmentally friendly, renewable, less harmful to living health, sustainable and cost-effective in the automotive industry would be increased by contribution of such studies.





2. PRELIMINARY WORK

2.1. Composites

Composite materials are made by combining at least two materials which have different properties, and these materials neither dissolve nor blend into each other. The purpose of combining two different material is to obtain unique properties which do not exist any of the material alone. (Ngo, 2020). Composites can be categorized according to reinforcement type, reinforcement material or matrix material. The categorization of these materials based on the reinforcement type is demonstrated in Figure 2.1.

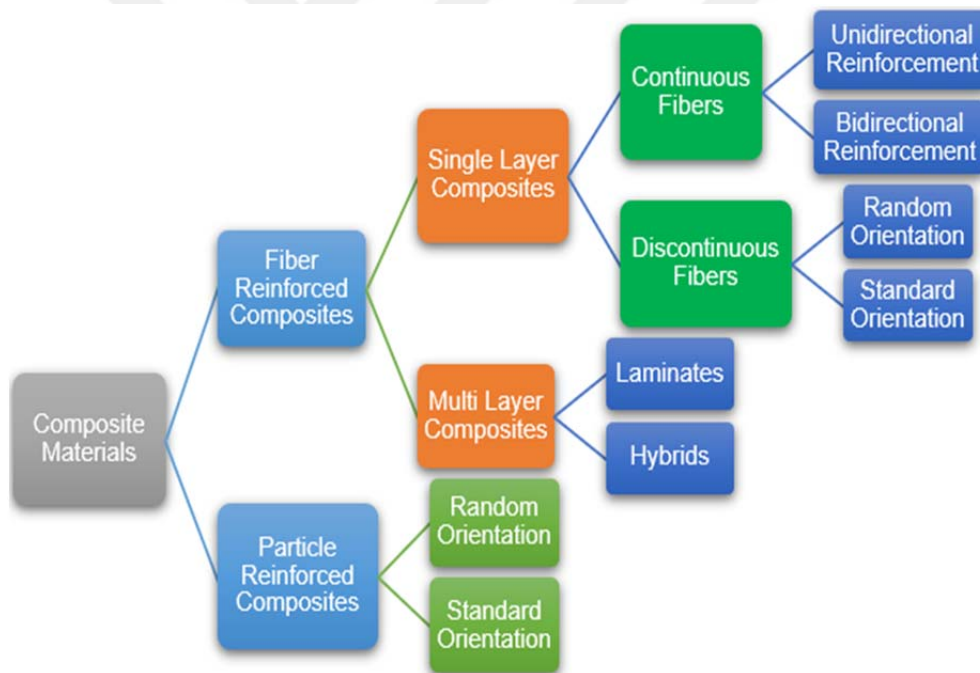


Figure 2.1. Categorization of composite materials (Kumar et al., 2022)

2.2. Hybrid Composites

Hybrid composites can be described as a combination of two or more different types of fibers within a single matrix. Hybrid composites are categorized as interply and intraply. Interply hybrids consist of one type of fiber per layer, while intraply hybrids consist of at least two types of fiber per layer (Sezgin, 2018).

Hybrid composites are generally designed for specific requirements. The properties of the hybrid composites can be changed and enhanced by altering the design of hybrid configuration. Two or more different fibers are brought together to take benefit of the properties of both fibers. By doing so, new materials that have improved additional properties could be produced (Agarwal et al., 2014). The strength of the hybrid composites depends on various factors such as the fiber property, the fiber length, the aspect ratio of fiber content, the fiber orientation, the bonding of fiber to the matrix interface etc. (Jawaid and Abdul Khalil, 2011).

The purpose of hybridization is to keep the advantages and minimize the disadvantages of fibers and reduce the cost (Dehkordi et al., 2010). In hybrid composites, one type of fiber usually has high modulus and high cost such as carbon, while the other type of fiber has low modulus and low cost such as glass fiber. Expensive and high modulus fibers enhance the stiffness of hybrid composites, while cheap and low modulus fibers reduce the cost and hybrid composites become more tolerant to damages (Safri et al., 2018).

Comprehensive studies have been conducted to enhance the performance of fiber reinforced hybrid composites and their applications. The studies based on synthetic and natural fiber reinforced hybrid composite materials have been discussed in this chapter.

Dehkordi et al. (2010), investigated impact properties of hybrid composites based on basalt and nylon woven fabrics. As a matrix material, epoxy resin was used in this study. Five different composite samples were produced with different volume percentages of nylon (0%, 25%, 33.3%, 50% and 100%) by using hand lay-up process. At several low velocity impact energy levels of 16 Joule (J), 30 J

and 40 J, the effect of nylon/basalt fiber content on residual deflection, maximum force and deflection, elastic energy, total absorbed energy, size and type of damage were examined. After the test, the results showed that an increase in nylon/basalt fiber ratio decreased the amount of maximum force. 100B (100% basalt fiber) laminate showed the highest maximum load and low contact duration, while 100N (100% nylon) sample had the least maximum load and high contact duration. Also, increasing the nylon fiber content in hybrid composites resulted in the laminates to become more ductile and less stiff. In addition, low nylon/basalt ratio caused fiber breakage, however, the damage spread to the extensive area by increasing the nylon fiber ratio. The results demonstrated that the basalt/nylon fibers ratio affects the impact behavior of hybrid composites significantly.

Ary Subagia et al. (2014), researched the effect of different stacking sequence of hybrid composites reinforced with carbon and basalt fibers. The vacuum-assisted resin transfer molding (VARTM) process was used to fabricate hybrid composite laminates, and as a matrix material, epoxy resin was preferred. Three-point bending test was performed to the hybrid composite laminates and the fracture surfaces was examined by Scanning Electron Microscopy (SEM). From the results, it was found that the flexural strength and modulus of the hybrid composites were dependent on the sequence of fiber reinforcement. When the mechanical properties examined, CFRP composite had the highest load (i.e., flexural strength) and showed low displacement. On the other hand, basalt fiber reinforced polymer (BFRP) composite had the lowest load and showed the largest displacement among all laminates. In addition, when carbon fiber layers were placed at the compressive side, the flexural strength and modulus of the hybrid composites increased compared to the basalt fiber being on the compressive side. The results suggested that the advantage of hybridization in this study is lesser cost, comparable flexural strength, and improved ductility compared to CFRP laminate.

Uzay et al. (2019), presented the impact strength of interply and intraply hybrid laminates based on carbon and aramid fibers. Epoxy resin was chosen as a

matrix material. In this study, four different composite laminates were fabricated with hand lay-up followed by vacuum bagging method. Two of the specimens were intraply and interply hybrid composites, and the others were pure laminates of aramid fiber fabrics and carbon fiber fabrics. Charpy impact test method was used to determine the amount of absorbed energy and impact strength of the fiber reinforced polymer (FRP) composites. The results indicated that pure carbon FRP composite showed the lowest impact strength and absorbed the minimum energy. Both intraply and interply hybrid composites had higher impact strength and energy absorption than pure FRP laminates. Briefly, hybridization of intraply laminates yielded better results compared to pure CFRP and aramid fiber reinforced polymer (AFRP) composites.

Karaçor and Özcanlı (2021), examined the mechanical properties of basalt, jute, and glass fiber reinforced hybrid composites by using various matrix materials. Six different hybrid composite laminates were produced by using vacuum-assisted resin transfer molding method. As matrix materials, epoxy and vinylester were preferred in this study. The mechanical properties of the hybrid specimens were obtained by the Tensile test and Vickers hardness test, while the morphology of the laminates were examined by SEM. It was found that the tensile strength of the basalt fiber/glass fiber (100 g/m²) reinforced with epoxy had the highest value among all the produced samples, while the jute/basalt fiber reinforced with epoxy had the lowest value. Also, epoxy reinforced basalt/glass fiber (100 g/m²) composites had 1.39 times higher hardness value than the vinylester reinforced basalt/glass fiber (100 g/m²) composites. In addition, all the composite samples produced with epoxy had higher Vickers hardness value than the samples produced with vinylester. SEM analysis results showed that there were less voids and more fiber breakage in the hybrid composites manufactured with epoxy resin than the composite samples manufactured with vinylester resin. When all the test results were considered, it was found that epoxy matrix reinforced hybrid

composites had superior performance than vinylester matrix reinforced hybrid composites.

Bandaru et al. (2016), studied the low-velocity impact (LVI) response of kevlar/basalt reinforced polypropylene (PP) composites. By using vacuum-assisted compression molding process with PP resin, three different composites (kevlar, basalt and hybrid combination of both) were produced. LVI tests were conducted at the energy level of 240 J by using drop-weight impact equipment, and then peak forces, energy absorptions and damage modes of the composites were compared. After the experimental tests, the results showed that B3D (three dimensional basalt) composites had the highest peak force, while H3D (three dimensional hybrid) composites absorbed more energy than other composites. In addition, experimentally induced damages of the composite samples were viewed by optical micrograph. It was observed that B3D composite sample had a smaller damaged area than K3D (three dimensional kevlar) composite sample, while the H3D hybrid sample showed the largest damaged area. The common failure mode in all composite specimens was fiber breakage in tension. In conclusion, it was observed that by hybridizing kevlar with basalt fibers enhanced the energy absorption and the damage tolerance.

Al-Hajaj et al. (2019), investigated the impact properties of hybrid composite materials made from carbon fibers and flax fibers in an epoxy matrix. Using hand lay-up followed by compression molding method, two types of hybrid composites, Type-A (unidirectional) and Type-B (cross-ply), were produced. A variety of impact energies (5-40 J) were applied to the hybrid composite specimens using a pendulum impact tester. The results showed that both composites demonstrated linear behaviour, but Type-B composite showed better energy absorbing capacity. Type-A and Type-B composites absorbed between 35 to 65% of the energy at 5-15 J of impact energy, while they absorbed between 70 to 84% of the energy at 20-30 J of impact energy. Images were taken of the front and the back faces of the Type-A and Type-B composites in order to evaluate failure

modes. On the back faces of both composites, there were no visual bulge deformation at an impact energy of 5 J. However, minor damages were observed on front and back faces of the plates at impact energy of 10 J. Also, at an impact energy of 40 J, close-up photos of plates showed fiber pull-out, fiber breakage and delamination. In conclusion, it was observed that Type-B composite had better performance as indicated by higher energy absorbing capacity, higher impact strength, smaller cracks and smaller damage areas compared to Type-A composite.

Ashraf et al. (2017), researched the mechanical behavior of woven/knitted hybrid composites of kevlar and glass yarn that produced with different stacking sequence. Epoxy resin was preferred as a matrix and composites were fabricated using hand lay-up method. Impact test, tensile test and dynamic mechanical analysis were carried out on fabricated composites. Impact test results showed that as the knitted percentage increases, more energy was required to break the samples due to the knitted fabrics having flexible structure. It was also obtained from these results that as the glass ratio increases the impact strength decreases. On the other hand, tensile test results indicated that knitted fabric percentage had a very prominent effect on tensile behavior. The tensile strength decreased as a result of the knit percentage increased. It was found that in order to achieve maximum tensile strength, hybrid samples should contain maximum glass percentage and minimum knitted percentage. When the dynamic mechanical analysis results were examined, the hybrid samples with higher knitted fabric ratios demonstrated lower storage modulus than the hybrid samples with higher woven ratios. In addition, storage modulus of the samples increased as the glass percentage increased. It was concluded that knitted fabric percentage had a direct effect on the impact strength, but tensile strength was not directly related to knitted percentage.

Randjbaran et al. (2014), examined the effects of stacking sequence layers of hybrid composites on ballistic energy absorption. Five different hybrid samples were manufactured from glass, carbon, and kevlar woven fabrics and epoxy resin by hand lay-up method (Table 2.1). The ballistic tests were run at the high-velocity

ballistic impact conditions using NIJ Standard 0801.01 as the experimental test setup. High-speed cameras were also used to calculate velocity.

Table 2.1. Fabricated composite plates from top surface to bottom surface (Randjbaran et al., 2014)

HYBRID 1	HYBRID 2	HYBRID 3	HYBRID 4	HYBRID 5
Kevlar	Glass	Kevlar	Glass	Kevlar
Carbon	Carbon	Glass	Kevlar	Carbon
Glass	Kevlar	Carbon	Carbon	Glass
Kevlar	Carbon	Glass	Carbon	Glass
Glass	Kevlar	Carbon	Glass	Carbon
Carbon	Glass	Kevlar	Kevlar	Kevlar

After all the tests were performed, the results showed that Hybrid 2 absorbed the maximum amount of ballistic energy by having 95,17 J, and Hybrid 1 absorbed the minimum by having 94,36 J. In addition, a positive linear relationship was observed between the size of damaged areas and kinetic energy. If the amount of absorbed ballistic energy is higher, the damaged area is larger. It was also seen that Hybrid 2 and Hybrid 4 showed similar behaviour in terms of the ballistic energy absorption and the final velocity. In conclusion, stacking the first layer with glass fiber demonstrated better result than using kevlar fiber. Moreover, it was observed from the results that using the combination of carbon and glass fiber in the central layers is more efficient.

Fiore et al. (2016), performed a study on flax and flax/basalt composite samples to assess the the influence of basalt-mat used as external layers on the durability behaviour of flax reinforced epoxy composites. In critical environmental conditions, long-term ageing tests were conducted on two different laminates. According to ASTM B 117 standard, both samples were exposed to salt-fog environmental conditions for 60 days and mechanically tested. Charpy impact tests

and quasi-static flexural tests were carried out according to ISO 179 standards and ASTM D 790 respectively. The experimental results demonstrated that the hybridization of flax with basalt fibers can be taken into account as a practical approach for improving the durability of natural fiber composites under salt-fog environment conditions.

2.3. Polymer Matrix Composites

Polymer matrix composites (PMC) are generated from polymer resins (thermosets, thermoplastics, or elastomers) with a reinforcement agent which are selected according to the required properties and applications. PMCs are one of the most popular composite types and they are used in large quantities for various composite applications. PMCs are generally preferred due to their low cost and easy manufacturing methods. Polyesters and vinyl esters are inexpensive and the most preferred polymer resins which generally used for GFRPs, while the epoxy resins cost more and widely utilized in PMCs for aerospace applications. Epoxies provide better mechanical properties in addition to moisture resistance in comparison to polyesters and vinyl esters. On the other hand, thermoplastic resins including polyetherimide (PEI), polyphenylene sulfur (PPS) and polyetheretherketone (PEEK) are promising materials to be used in aerospace applications in the future (Callister, 2007).

2.3.1. Matrix Material

The function of the matrix is to bind fibers in an order and to protect them from environmental effects. The matrix plays an important role in transferring loads to fibers in addition to preventing premature defects owing to fiber micro buckling in compression loadings. Furthermore, the matrix can also provide the composite with various properties such as toughness, impact resistance, wear resistance and damage tolerance. In addition, resistance to moisture, thermal stability and maximum usage temperature are signified by the properties of matrix.

For advanced composites, polymeric matrices can be classified as thermosets and thermoplastics (Campbell, 2010).

2.3.1.1. Thermosets

One of the most widespread matrices in composites are thermosets due to having good fiber impregnation, low viscosity and low process temperatures. In addition, they generally cost less than thermoplastics (Lee and Suh, 2006).

There are various thermoset resins including epoxies, vinyl esters, polyesters, polyimides, bismaleimides, phenolics and cyanate esters. Thermoset resins have low viscosity monomers which are transformed into cross-linked structures during curing (Campbell, 2010).

At room temperature, thermoset resins show brittle behavior and cannot be reshaped by adding heat due to having crosslinks. Moreover, they decompose during reheating process and are able to burn in some conditions. Thermoset resins are able to be used at higher temperatures and show more resistance to chemical attacks compared to most thermoplastics (Lee and Suh, 2006).

2.3.1.2. Thermoplastics

Thermoplastics are comparatively soft and flexible, also they are able to become more flexible and softer after heating process. Unlike thermosets, thermoplastic materials do not form crosslinks and have linear or branched-chains (Bolton, 1993).

Thermoplastics are able to be reprocessed due to not having crosslinks. For instance, thermoplastics can simply be thermoformed by reheating to the process temperature. However, there is a limitation in thermoplastic reprocessing owing to the processing temperature and the degradation temperature of polymer are close. Eventually, the resin would degrade after multiple reprocessing and it can also crosslink in some instances. Thermoplastics are significantly tougher than thermosets because they do not have crosslink structure (Campbell, 2010).

The well-known thermoplastics commercially available for composites are polystyrene, polyethylene terephthalate (PET), polypropylene, polyamide (PA), polybutylene terephthalate (PBT), polyetherether ketone (PEEK) and polyphenylene sulfide (PPS) (Campbell, 2010).

2.4. Reinforcement

In general, composites are manufactured with a reinforcement material in addition to a matrix material. These reinforcements are whiskers, particles and fibers. Particles do not have preferred orientation and are generally used as fillers in order to lower the price of materials. They provide little improvements in terms of mechanical properties. On the other hand, whiskers are very strong single crystals, however it is difficult to spread them out evenly in the matrix. Fibers are predominantly used for advanced composite applications due to having the stiffness and strength advantages (Campbell, 2010).

Fibers are divided into two groups as synthetic and natural fibers. Synthetic fibers such as glass, aramid (kevlar) and carbon are the main reinforcements preferred in composite manufacturing. Carbon and aramid fibers are frequently utilized since they offer high strength and stiffness, while E-Glass fibers are preferred owing to their low cost. Recently, natural fiber usage in composite fabrication is progressively increasing (Shahzad, 2009).

Natural fibers are able to be derived from animals, minerals and plants. Natural fibers have advantages such as being renewable and inexpensive compared to synthetic fibers. Due to the environmental awareness and strict regulations by governments to reduce emissions, natural fibers are progressively preferred rather than synthetic fibers (Xueyuan, 2015). The classification of natural fibers based on their origin is presented in Figure 2.2.

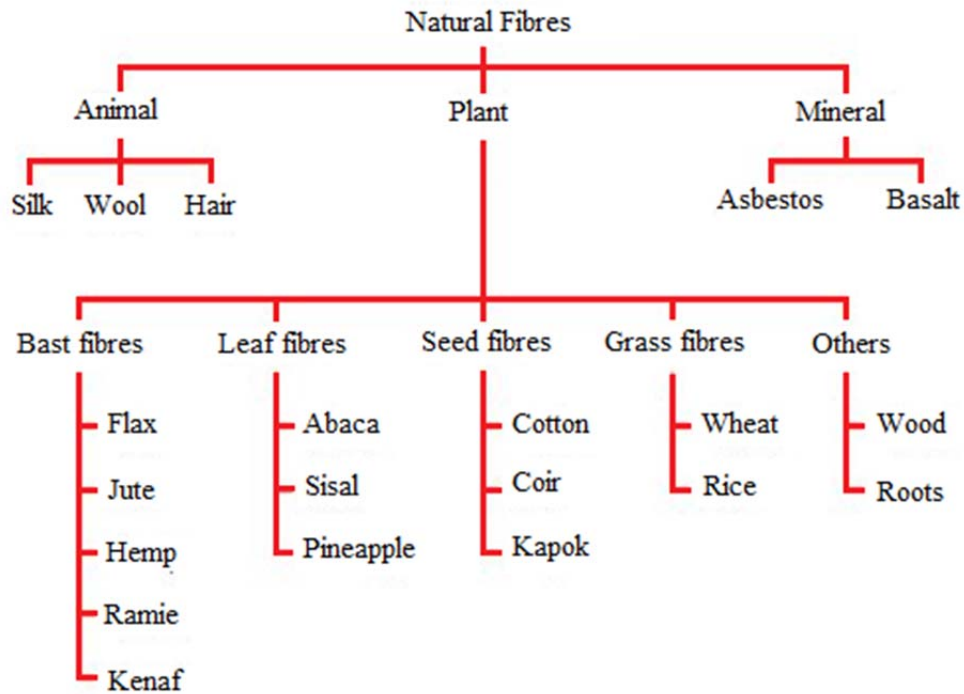


Figure 2.2. Types of natural fibers classified by source of their origin (Pornwannachai, 2015)

2.5. Manufacturing Methods of Composites

The selection of a composite fabrication process is heavily determined by the physical or chemical characteristic of a matrix (Lee and Suh, 2006). Composite samples are able to be fabricated with various manufacturing techniques than the conventional ones and this is one of the disadvantages of composite usage (Serin et al., 2019). There are various composite manufacturing methods and they are demonstrated in Figure 2.3.

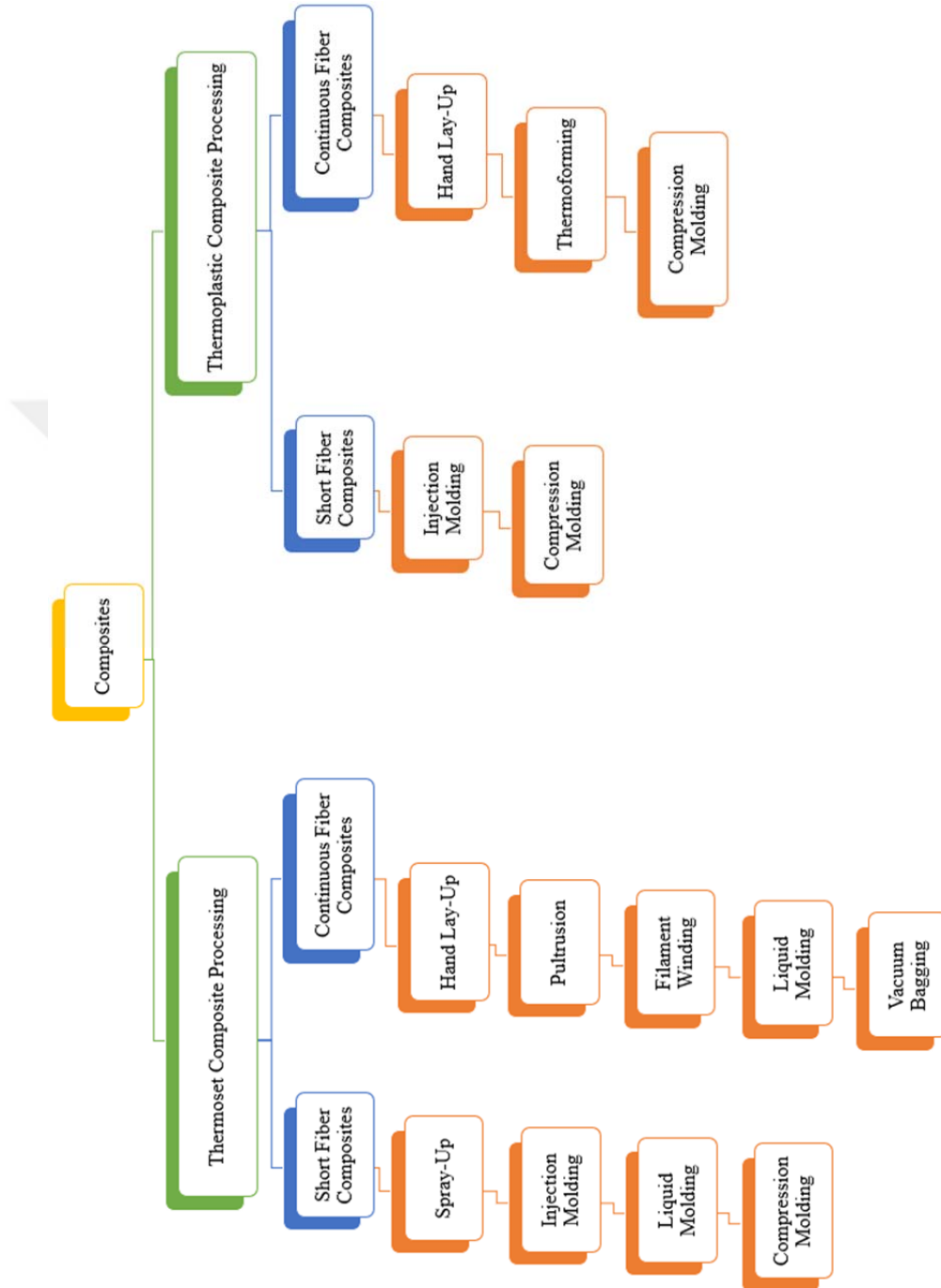


Figure 2.3. Composite processing techniques (Campbell, 2010)

2.5.1. Hand Lay-Up

Hand lay-up is oldest and simplest fabrication method for PMCs. In this method, fiber layers are stacked by hand, then the resin is impregnated via a roller (Figure 2.4). The tooling cost of this method is low and one can manufacture complex shaped products with this method. Due to these advantages of hand lay-up process, the manufacturers prefer to use this technique. In addition, one of the most preferred technique is hand lay-up for prototyping of composite products. In order to control the curing process, this method is combined with autoclave in some applications (Sureshkumar et al., 2014, Munawar et al., 2016, Cui et al., 2016, Nandaragi et al., 2018, Thippesh, 2018).

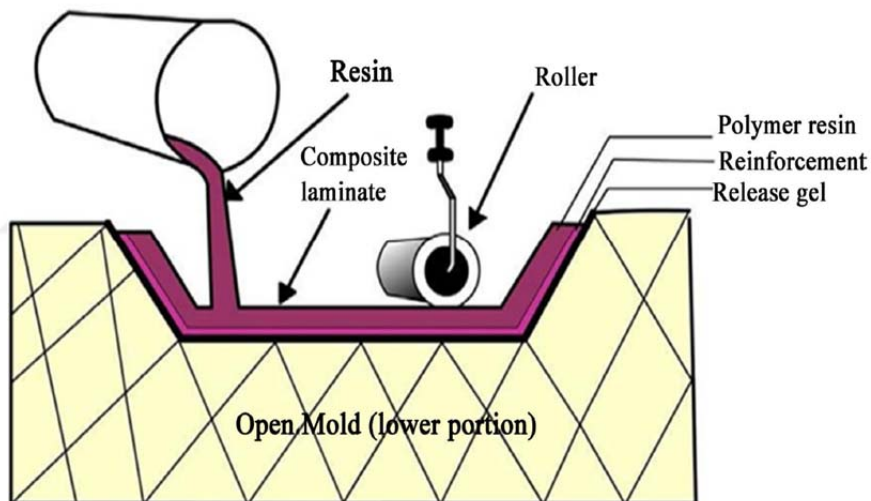


Figure 2.4. Typical hand lay-up process (Palle et al., 2022)

2.5.2. Filament Winding

Filament winding is a classic manufacturing technique that is well suited to the automated production process. In this method, continuous fiber rovings are crossed the comb device that is able to collect and assemble the fiber bundles. Then, fiber strands are passed through a resin bath and completely impregnated.

Fiber rovings are wound on a mandrel in different fiber orientation (Quanjin et al., 2019). Filament winding process is demonstrated in Figure 2.5.

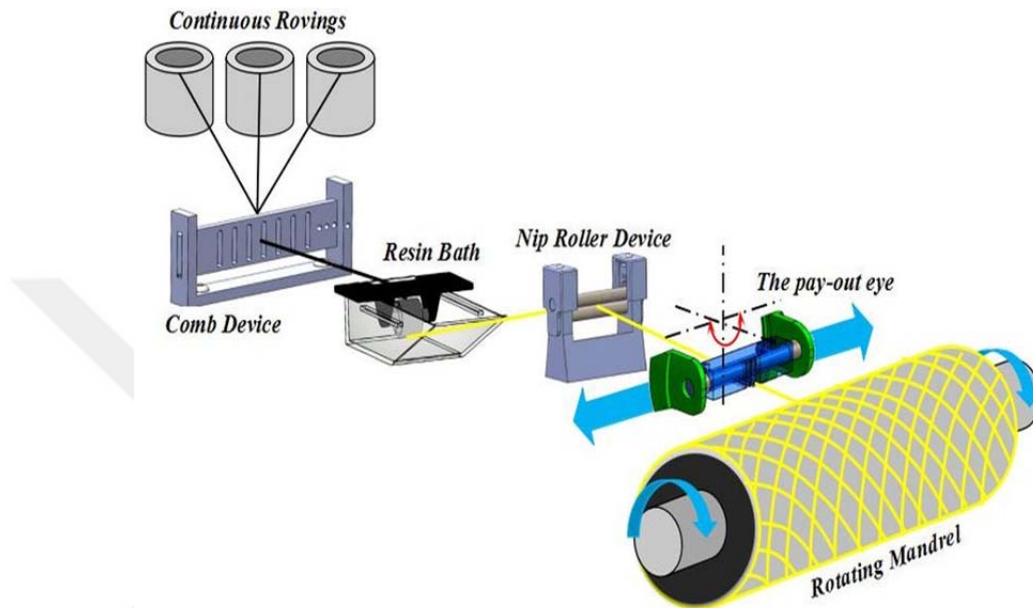


Figure 2.5. Schematic of filament winding process (Quanjin et al., 2019)

2.5.3. Vacuum Bagging

Vacuum bagging is an advanced method which can be used with hand lay-up in order to remove trapped air. A vacuum bag is used to cover the mold, then the mold is vacuumed (Figure 2.6). Thus, the air inside the mold is extracted by vacuum process (Hall and Javanbakht, 2021). The aviation and space industry are the main usage area of this method due to the importance of the performance of composite parts (Lee and Suh, 2006).

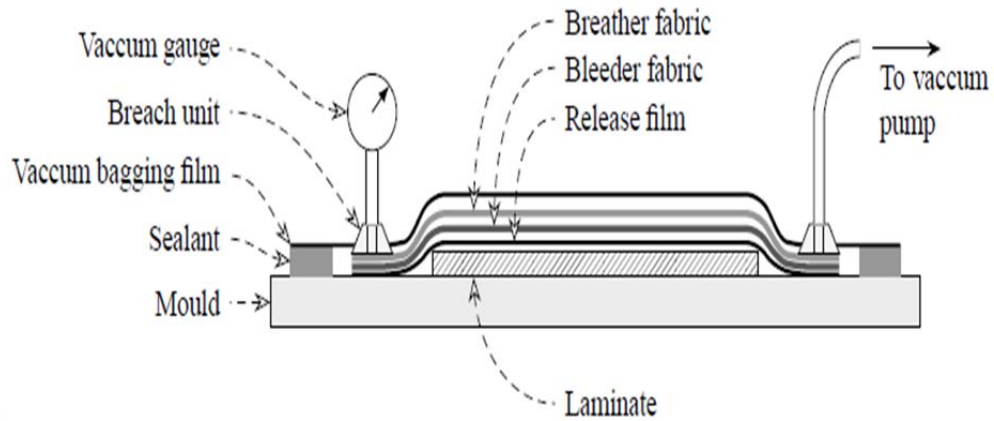


Figure 2.6. Schematic of vacuum bagging process (Hall and Javanbakht, 2021)

2.5.4. Pultrusion

Pultrusion is a method that is similar to extrusion. In this method, fiber wicks are immersed into a resin bath and pulled out from a forming die (Figure 2.7). The widely used resin types in pultrusion are epoxies, unsaturated polyesters and all thermosetting polymers (Groover, 2010).

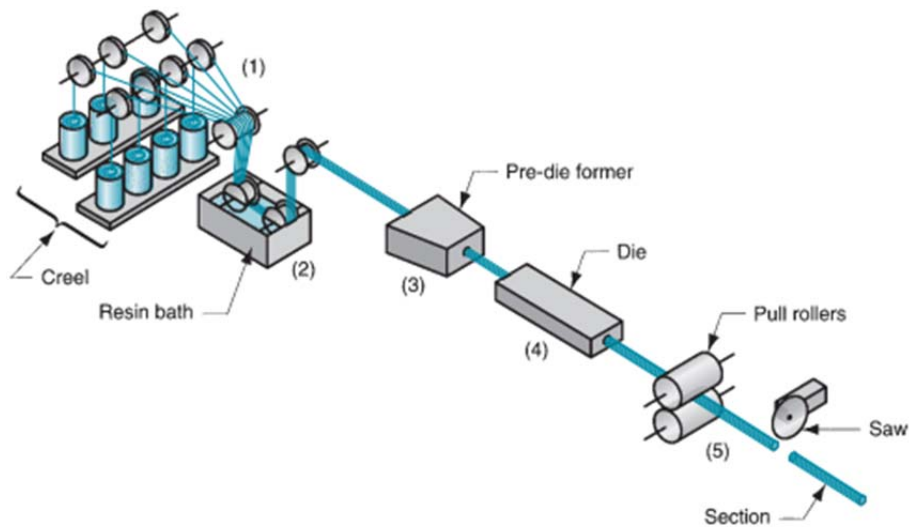


Figure 2.7. Pultrusion process (Groover, 2010)

2.5.5. Resin Transfer Molding

Resin transfer molding (RTM) is a composite manufacturing process which is used for mass production of structural parts using continuous fibers and thermosets with low viscosity. In 1980s, RTM was adopted for composite manufacturing in order to achieve the mass production of structural parts in the automotive industry (Advani and Hsiao, 2012).

RTM is a reactive polymer processing technique where liquid reactants toughen in a mold. The mold contains fiber reinforcements in order to manufacture a composite part. In RTM, a resin is mixed via a static mixer at low pressure, then it is pumped into the mold. The filling pressure of the mold is usually below 0.7 MPa for RTM and the required force for compression of the mold is low. (Lee and Suh, 2006). Figure 2.8 demonstrates a diagram of the different stages of the RTM process.

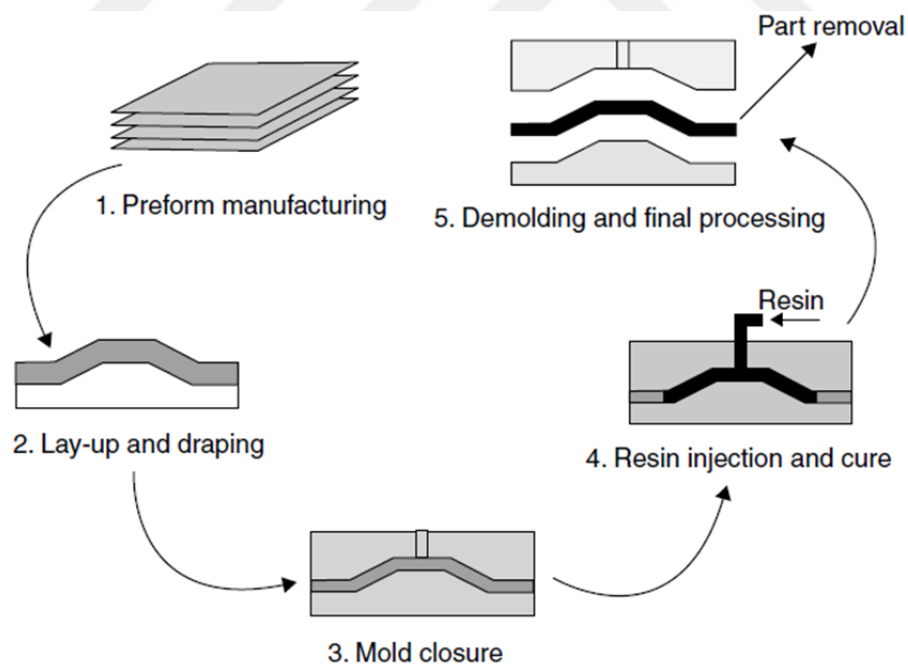


Figure 2.8. RTM process (Advani and Hsiao, 2012)

2.5.6. Vacuum Infusion

The vacuum infusion method is a closed mold process and large-scale parts with high performance can be produced using this method. Vacuum infusion has a key role in enhancing the quality and the cost of large composite structures. (Advani and Hsiao, 2012). A vacuum pressure is used for injection and curing in this method. The design of vacuum infusion is much simpler and cheaper than RTM method. Recently, the attention of aviation industry is progressively increasing for usage of vacuum infusion process (Campbell, 2010).

In general, vacuum infusion can be summarized in five stages: (1) the preparation of the mold and the placement of fabrics; (2) sealing the mold with a tape and creating a vacuum; (3) the preparation of resin; (4) the impregnation of resin and (5) the curing of manufactured laminates (Ary Subagia et al., 2014). A typical vacuum infusion method is demonstrated in Figure 2.9.

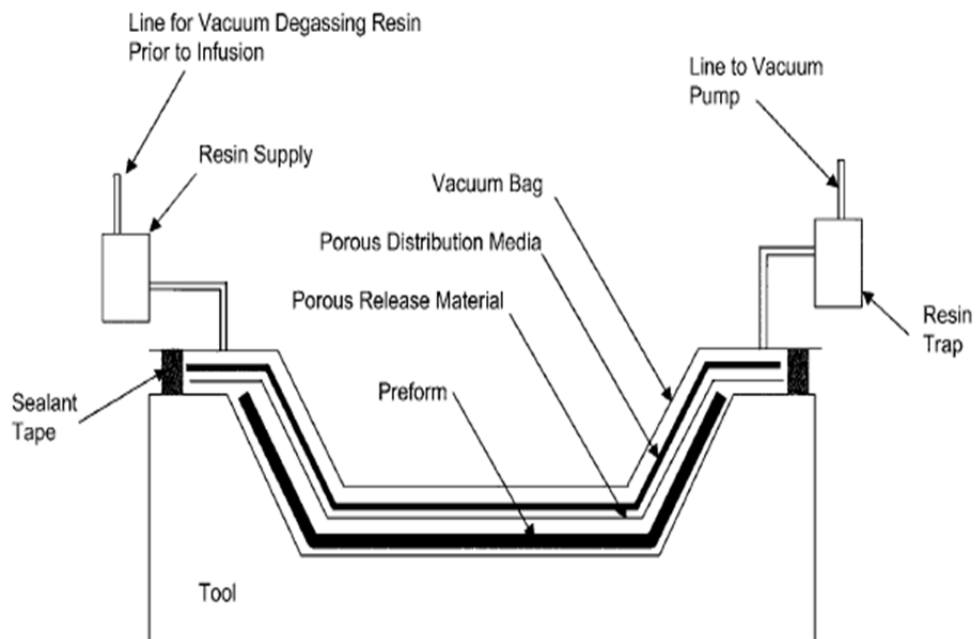


Figure 2.9. Typical vacuum infusion method (Campbell, 2010)



3. MATERIAL AND METHOD

3.1. Materials

3.1.1. Carbon Fiber

Carbon fibers are a new type of high strength materials made from graphitic and non-crystalline regions. Among of all reinforcing fibers, carbon fibers are the ones that offer the highest specific modulus and strength. Carbon fibers also offer high electrical and thermal conductivities with a relatively low coefficient of thermal expansion (Prashanth et al., 2017).

Carbon fibers are resistant to many chemical solutions that do not absorb water. They are perfectly resistant to fatigue, do not cause corrosion, do not show any relaxation. They show less relaxation than low slackening high tension prestressed steel strips. Carbon fiber is electrically conductive and can therefore cause galvanic corrosion in direct contact with steel (Carolin, 2003).

The two main sectors of carbon fiber applications are high-tech sectors including aviation, nuclear engineering; and general engineering and transport, including automobile bodies, engineering components. However, the requirements of the two sectors are fundamentally different. Large scale use of carbon fiber airplanes and aviation in terms of maximum performance and fuel efficiency are crucial, while the cost factor and production requirements are not critical. The use of carbon fibers in general engineering and transportation is dominated by cost constraints, high throughput requirements and generally less critical performance requirements (Chand, 2000).

3.1.2. Aramid Fiber (Kevlar)

Kevlar is an aramid fiber of Poly-para-phenylen-terephthalamide (PPTA) with a rigid molecular structure. Aramid like fibers were first developed in 1960s as an alternate for steel reinforcements in rubber tyres. However, once developed the aramid fibers were also found suitable for ballistics and as surrogate for

asbestos. Kevlar fibers are often used for high-performance composite applications where light weight, high strength and stiffness, damage resistance, and resistance to fatigue are of utmost importance. Aramid fibers are often employed in those applications that demands high strength and low weight together with a high impact resistance. Some of the most frequent applications of aramid materials include bullet proof vests, cooling vehicles, ship hulls and lately towards structural strengthening of civil structures. Nevertheless, aramid fibers often present low compression strength. Further, the compressive modulus of aramid is of the same order as its tensile modulus. In general, aramid fibers are grouped into two categories: meta-aramid and para-aramid.

Meta-aramid fibers often present excellent thermal, chemical and radiation resistance. They are usually employed in the fabrication of fire-retardant textiles such as outer wear for fire fighters and racing car drivers.

Para-aramids fibers offer higher strength. These are more commonly used in fibers reinforcement plastics for engineering structures, stress skin panels, and other high tensile strength applications. Kevlar and Technora are commercially important para-aramid fibers (Prashanth et al., 2017).

3.1.3. Basalt Fiber: Basalt is a volcanic extrusive mineral obtained by a rapid cooling of the melted lava. Basalt rocks are widespread on the earth's crust and, even if they can differ by chemical composition in dependence on the geographical site of formation, they generally show good properties in terms of both chemical, physical stability and mechanical properties (Scalici et al., 2016; Colombo et al., 2012; Novitskii and Efremov, 2013)

The procedure to extrude fibers by processing basalt rock is relatively old and it took research work throughout all the second half of last century to obtain an optimized process and competitive final product. Nowadays basalt fibers for the composite manufacturing industry are available and obtained with processes similar to those employed for glass fibers, but generally easier and with lower

environmental impact. These achievements, together with the nominally superior stiffness and strength properties in addition to good thermal and chemical stability, have proposed basalt fibers as an appealing alternative to glass fibers. Furthermore, despite the similarity in chemical composition with asbestos, basalt fibers do not cause health risks and they have been successfully used as reinforcement for thermosetting and thermoplastic matrix resin systems (Scalici et al., 2016). The physical and mechanical properties of basalt fiber compared to synthetic fibers are demonstrated in Table 3.1.

Table 3.1. Properties of Basalt fiber and synthetic fibers (Militký et al., 2018)

Properties	Basalt	E-glass	S2-glass	Aramid	Carbon
Density (kg/m ³)	2630–2800	2540–2570	2540	1450	1780–1950
Filament diameter (µm)	6–21	6–21	6–21	5–15	5–15
Single filament tensile strength (MPa)	3000–4840	3100–3800	4020–4650	2900–3450	3500–6000
Initial modulus (GPa)	93–110	72.5–75.5	83-97/86	70–140	230–600
Elongation at break (%)	3.1–6	4.7	5.3	2.8–3.6	1.5–2.0

In general, the positive features of this new generation of basalt fibers include sound insulation properties, excellent heat resistance (better than glass), good resistance to chemical attack and low water absorption. For the latter reason they are suggested for applications requiring thermal insulation as well as for hot fluids transportation pipes. Another important characteristic is represented by the high mechanical performance comparable to that of glass fiber, that together with the lower cost could make this material suitable to potentially replace glass fibers in various industrial fields like aerospace, automotive, transportation and

shipbuilding (Lopresto et al., 2011). The average price (converted from Turkish Lira to United States Dollar) of basalt fiber compared to synthetic fibers are shown in Figure 3.1.

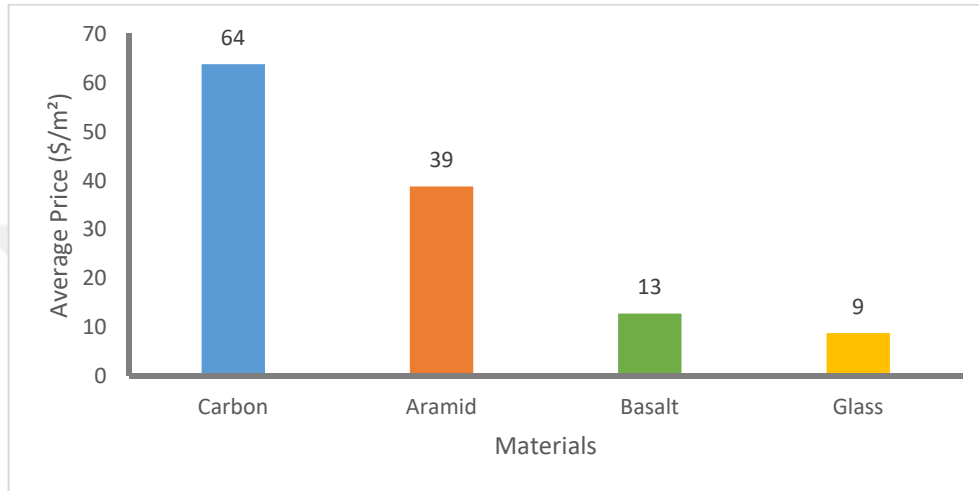


Figure 3.1. Price comparison of Basalt fiber and synthetic fibers (Kompozitshop, 2022)

In this study, carbon fiber, aramid fiber and basalt fiber (country of origin: Istanbul, Turkey for all fabrics) were used as a reinforcement material. Reinforcement properties were shown in Table 3.2 (Kompozitshop, 2020). Fabric samples used in the study can be seen in Figure 3.2.

Table 3.2 Properties of fabrics

Fabric	Weave	Weight (g/m ²)	Thickness (mm)	Density (g/cm ³)	Warp x Weft (micron)
Carbon	Twill	245	0,25	1,79	7 x 7
Aramid	Twill	170	0,2	1,4	6,7 x 6,7
Basalt	Plain	210	0,19	2,75	12 x 12

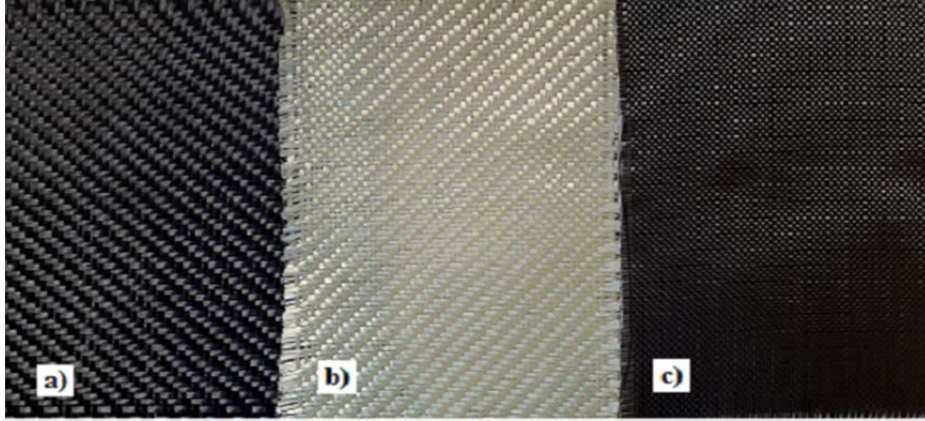


Figure 3.2. Fabric samples respectively; a) Carbon fiber (245 g/m²), b) Aramid fiber (170 g/m²), c) Basalt fiber (210 g/m²)

3.1.4. Matrix Materials

Matrix materials are in liquid form and can be cured at room temperature. In accelerator LR160 (country of origin: Istanbul, Turkey) and as a hardener in LH160 (country of origin: Istanbul, TURKEY) created the epoxy resin mixture for the matrix material system.

L160 Infusion epoxy resin systems are the products used in aviation, automotive, marine, aerospace, wind propellers and defense industries, which are widely used in advanced composite parts manufacturing in the world. The L160 system, which has aviation certificate, can be easily used in infusion applications that are not very large. It cures at room temperature and parts that meet civil aviation standards can be obtained by post curing. Properties of epoxy and hardener were given in Table 3.3 (Kompozitshop, 2019).

Table 3.3. Epoxy and hardener properties

	LR160 Infusion Epoxy	LH160 Hardener
Operating temperature (° C)	-60 / +50 without heat treatment -60 / +80 by applying heat treatment	-
Process temperature (° C)	+10 / +50	-
Density (g / cm³)	1,13-1,17	0,96-1,00
Viscosity (mPas)	700-900	10-50
Refractor index	1,5480-1,5530	1,5200-1,5210
Amine value (mg KOH / g)	-	550-650
Measurement Conditions	25°C	25°C

3.2. Method

3.2.1. Preparation Process of Matrix Materials

One of the most important points to be considered in the manufacture of composites is to determine the mixing ratios of matrix materials. These rates were prepared as 100: 25 ±2 by weight according to the manufacturer's specifications. If these chemicals are used less than necessary, they will defect the manufactured product, which will prevent the adherence of the fabric and resin and harden the sample. On the other hand, using it more than necessary may cause the resin to solidify.

3.2.2. Manufacturing of Composite Materials

In this study, five different types of composites were produced for each test. In total, twenty-five different fabric-reinforced composite materials were produced using this method. Five of these were pure carbon fiber-reinforced

composites, while the other twenty were hybrid composite structures of aramid and basalt fiber. Sample codes were given to these materials according to first letter of the fiber which is A for aramid, B for basalt, C for carbon, and the numbers next to letters indicate the layer number of the fibers as in Table 3.4. In addition, fiber layouts of composite materials are shown with different colors for each fiber in Table 3.5, 3.6, 3.7 and 3.8.



Table 3.4. Composite codes and composite contents of produced materials

Composite Codes	Composite Contents
C9	9 layers of carbon fiber
B8A4	8 layers of basalt fiber and 4 layers of aramid fiber, basalt fibers on the top and at the bottom surfaces
A4B8	4 layers of aramid fiber and 8 layers of basalt fiber, aramid fibers on the top and at the bottom surfaces
B6A6	8 layers of basalt fiber and 4 layers of aramid fiber, basalt fibers on the top and at the bottom surfaces
A6B6	6 layers of aramid fiber and 6 layers of basalt fiber, aramid fibers on the top and at the bottom surfaces
C44	44 layers of carbon fiber
A17B32	17 layers of aramid fiber and 32 layers of basalt fiber, aramid fibers on the top and at the bottom surfaces
B32A17	32 layers of basalt fiber and 17 layers of aramid fiber, basalt fibers on the top and at the bottom surfaces
A24B24	24 layers of aramid fiber and 24 layers of basalt fiber, aramid fibers on the top and at the bottom surfaces
B24A24	24 layers of basalt fiber and 24 layers of aramid fiber, basalt fibers on the top and at the bottom surfaces
B6A3	6 layers of basalt fiber and 3 layers of aramid fiber, basalt fibers on the top and at the bottom surfaces
A3B6	3 layers of aramid fiber and 6 layers of basalt fiber, aramid fibers on the top and at the bottom surfaces
B5A4	5 layers of basalt fiber and 4 layers of aramid fiber, basalt fibers on the top and at the bottom surfaces
A4B5	4 layers of aramid fiber and 5 layers of basalt fiber, aramid fibers on the top and at the bottom surfaces
C7	7 layers of carbon fiber
B4A3	4 layers of basalt fiber and 3 layers of aramid fiber, basalt fibers on the top and at the bottom surfaces
A3B4	3 layers of aramid fiber and 4 layers of basalt fiber, aramid fibers on the top and at the bottom surfaces
B3A4	3 layers of basalt fiber and 4 layers of aramid fiber, basalt fibers on the top and at the bottom surfaces
A4B3	4 layers of aramid fiber and 3 layers of basalt fiber, aramid fibers on the top and at the bottom surfaces

Table 3.7. Composite codes and fiber layouts for Water Absorption test

Composite Codes	Fiber Layouts
C9	■ ■ ■ ■ ■ ■ ■ ■ ■ ■
B6A3	■ ■ ■ ■ ■ ■ ■ ■ ■ ■
A3B6	■ ■ ■ ■ ■ ■ ■ ■ ■ ■
B5A4	■ ■ ■ ■ ■ ■ ■ ■ ■ ■
A5B4	■ ■ ■ ■ ■ ■ ■ ■ ■ ■

■ : Carbon Fiber, ■ : Basalt Fiber, ■ : Aramid Fiber

Table 3.8. Composite codes and fiber layouts for Loss on Ignition test

Composite Codes	Fiber Layouts
C7	■ ■ ■ ■ ■ ■ ■ ■ ■ ■
B4A3	■ ■ ■ ■ ■ ■ ■ ■ ■ ■
A3B4	■ ■ ■ ■ ■ ■ ■ ■ ■ ■
B3A4	■ ■ ■ ■ ■ ■ ■ ■ ■ ■
A4B3	■ ■ ■ ■ ■ ■ ■ ■ ■ ■

■ : Carbon Fiber, ■ : Basalt Fiber, ■ : Aramid Fiber

These parts were produced in Cukurova University Automotive Engineering Laboratories with vacuum infusion method. Composite fabrication was carried out at room temperature ($20^{\circ}\text{C} \pm 2^{\circ}\text{C}$). The production steps of this system from Figure 3.3 to 3.9 were shown.

Production stages were as follows:

- I. First, the surface was cleaned with a substance such as thinner.
- II. A layer of mold separator material was applied to the surface, if necessary, a second layer can be applied after fifteen minutes.

- III. The fabrics were laid on the surface in the specified order, then peel ply and infusion mesh was placed at the end, respectively.
- IV. Infusion and vacuum hoses were attached to the infusion mesh with a sealant tape to stabilize the position of the laid fabrics and to ensure a homogeneous resin flow.
- V. The frame was determined by vacuum sealing tape. Two hoses were fixed to the frame as the input and the output.
- VI. The vacuum bag was carefully installed around the frame to prevent air leak.
- VII. The vacuum pump was run to test for air leak.
- VIII. Simultaneously, resin mixture was prepared in the calculated amount and the vacuum machine was run.
- IX. When the pressure gauge reached -760 mm-Hg, the infusion was continued until the entire surface got wet.
- X. The vacuum pump was operated until it absorbed the required amount of resin, the vacuum pump and all holes must be closed when the process was finished.
- XI. After waiting 24 hours in this position for the sample to cure, the vacuum bag opened and the infusion mesh, peel layer was separated from composite sample. The manufactured composite samples were kept in the oven for 1 hour at 60 ° C. The production stages mentioned were demonstrated below.



Figure 3.3. The cleaned surface area determined by vacuum sealing tape



Figure 3.4. Mold release wax applied to the surface



Figure 3.5. Vacuum hoses attached to system and layered fabrics were placed in frame



Figure 3.6. Peel ply laid on the sample



Figure 3.7. Infusion mesh laid on the sample



Figure 3.8. Vacuum bag attached to system and air inside the system vacuumed

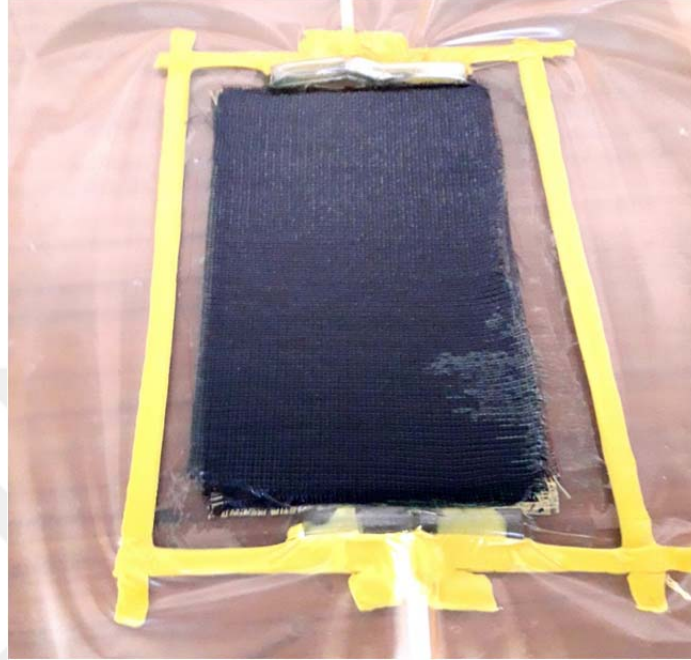


Figure 3.9. Fully resin impregnated material

3.2.3. Experimental

3.2.3.1. Tensile Test Analysis

In this study, the mechanical characteristics of the composite specimens were scrutinized by tensile strength. Dimensions of the tensile test specimen according to ASTM D 3039 standard is demonstrated in Figure 3.10. Five samples were tested for each produced C9, A4B8, B8A4, A6B6, and B6A6 composites (Figure 3.11). Tensile testing was conducted at room temperature using ALŞA Hydraulic Test Machine (KOLUMAN Automotive Industry Laboratory) according to the ASTM D 3039 standard and the crosshead speed was set as 2 mm/min using a capacity of 100 kN load cell. Tensile test machine is shown in Figure 3.12. As a result; tensile strength, elastic modulus, stress-strain diagram and elongation rate of the hybrid composites were calculated.

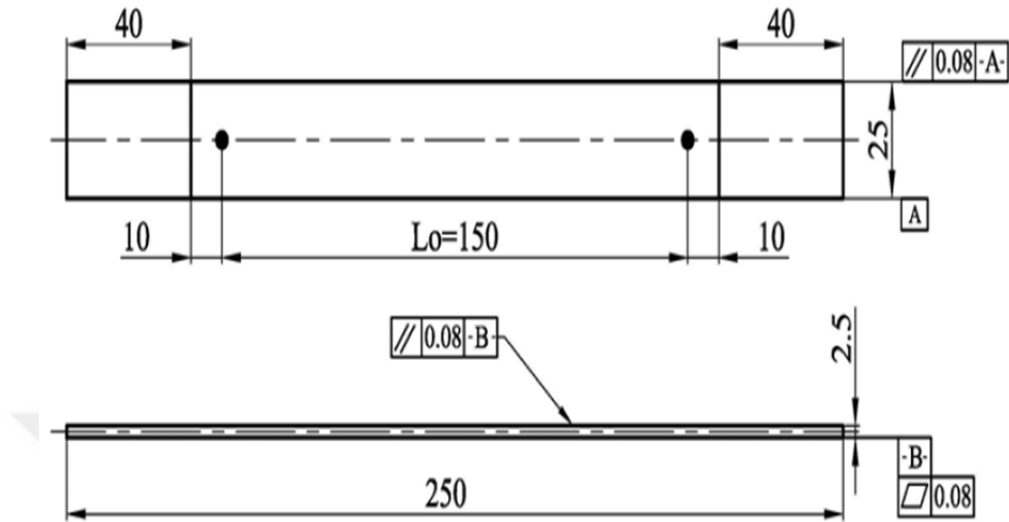


Figure 3.10. Dimensions of the tensile test specimen according to ASTM D 3039 standard (Alarifi, 2021)

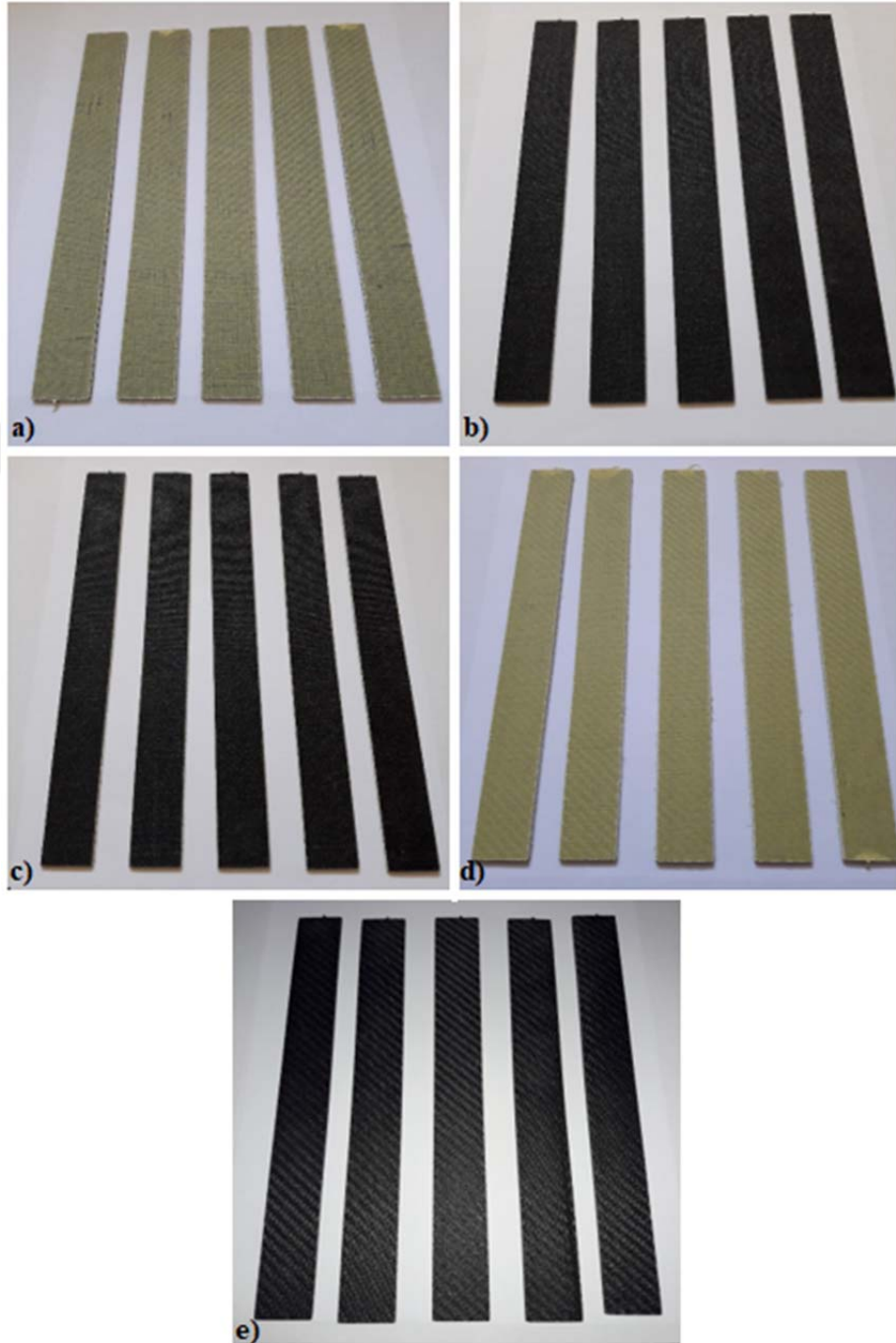


Figure 3.11. Tensile test specimens; a) A4B8, b) B8A4, c) B6A6, d) A6B6, e) C9

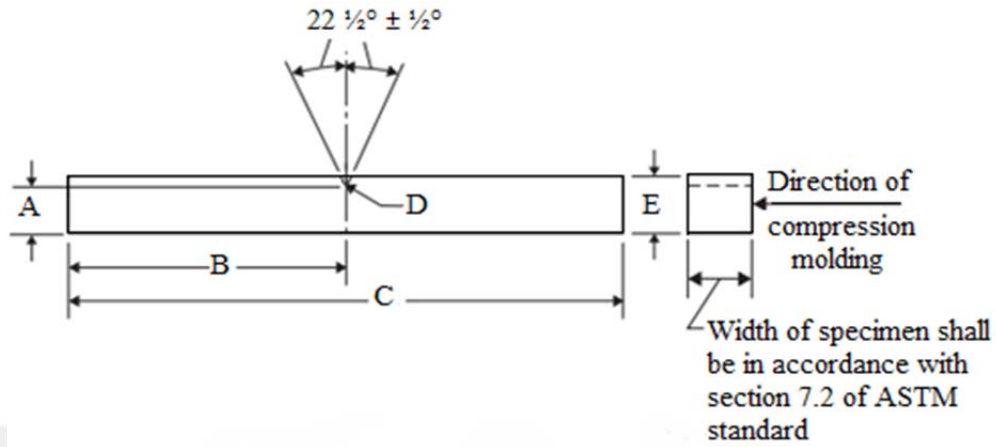


Figure 3.12. Tensile testing machine

3.2.3.2. Impact Test Analysis

The Charpy impact test measures the energy absorbed by a standard notched sample as it breaks under an impact load. This absorbed energy shows a measure of the notch toughness of the material being tested and acts as a tool to study the ductile-brittle transition depending on the temperature.

For the Charpy Impact Test, a rectangular sample with a sample size of 125x 12.5x 10 mm was prepared according to the ASTM D 6110 standard, with a 2.0 mm 'V' notch per sample and an angle of 45 ° (Figure 3.13) and produced composite materials are shown in Figure 3.14. Fifteen composite samples were taken from the products produced for the analysis of impact resistance. The notches were opened in the middle of each sample with a notch opening device in the Mechanical Engineering Laboratory of Cukurova University (Figure 3.15).



A	10.16 ± 0.05	0.400 ± 0.02
B	63.5 max. 61.0 min.	2.50 max. 2.40 min.
C	127.0 max. 124.5 min.	5.0 min. 4.90 min.
D	0.25R ± 0.05	0.010R ± 0.002
E	12.70 ± 0.15	0.500 ± 0.006

Figure 3.13. Dimensions of Charpy type test specimen (Ashter, 2014)

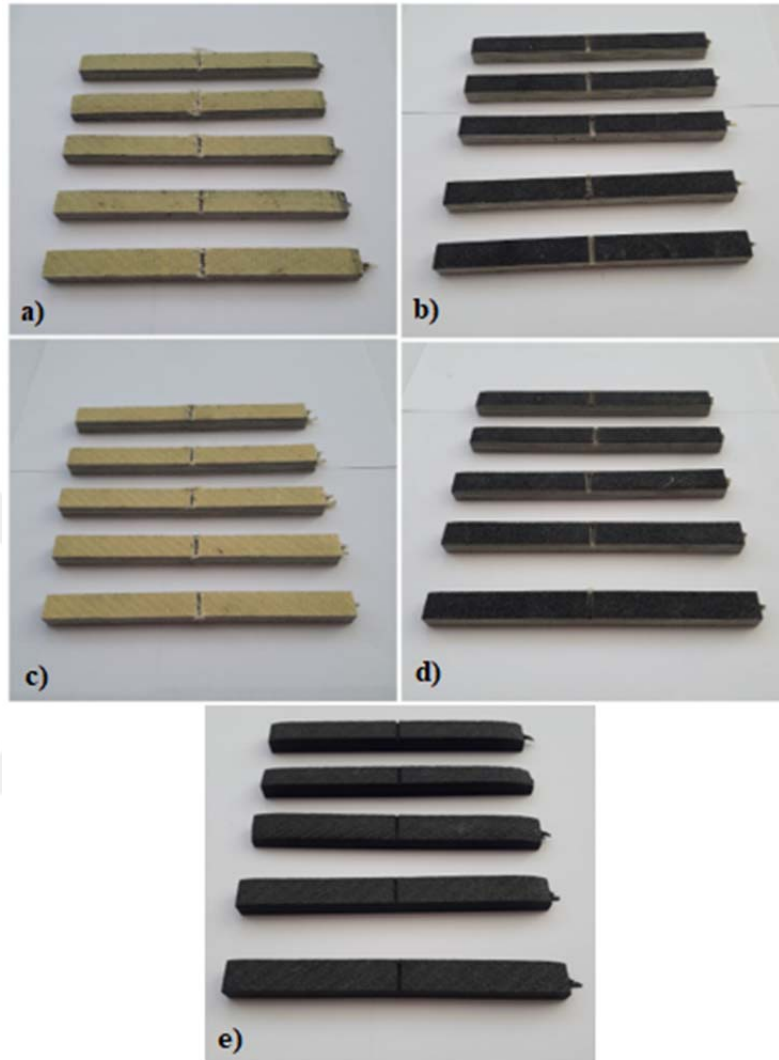


Figure 3.14. Composite material samples which produced for Charpy impact test;
a) A17B32, b) B24A24, c) A24B24, d) B32A17, e) C44



Figure 3.15. Notching device

ALŞA Charpy Impact Testing Machine was used to measure the impact resistance of the samples prepared according to the ASTM D 6110 standard (Figure 3.16). Impact test was conducted at Mechanical Engineering Laboratory of Osmaniye Korkut Ata University. The specification of the test machine was presented in Table 3.9.

Table 3.9. Specification of Charpy Impact Testing Machine

Model	450 CE
Hammer Weight (kg)	30.7
Hammer Height (mm)	770
Angle of Hammer (degree)	160 °



Figure 3.16. Impact testing unit

In this test, the sample was safely held at both ends, giving the energy value absorbed by the sample by multiplying the hammer in a pendulum arm by the sample made according to the standards. The hammer hits against the notch in the sample being produced. The energy absorbed by the sample is decided by precisely measuring the decrease in the movement of the pendulum arm (Mohammad et.al 2019).



Figure 3.17. Sample placed to test region

The composite samples were placed in the machine as shown in Figure 3.17, and the analysis was done in this way after part placement for each sample tested. The results of the analysis were recorded from the data on the screen of the device (Figure 3.18).



Figure 3.18. Data screen of Charpy impact test machine

After analysis, impact strength can be calculated from the following equation:

$$\text{Impact strength} = E/t \times 1000 \quad (3.1)$$

‘E’-Energy used to break(J)

‘t’-Thickness in mm (Sakthivel and Rajendran, 2014).

3.2.3.3. Morphological Analysis

The purpose of this analysis is to examine the interfacial morphologies of the composite samples with the help of a Scanning Electron Microscope FEI Quanta 650 Field Emission device at 100V-30kV acceleration voltage. The machine seen in Figure 3.19 has a magnification capacity of 6-1,000,000 times. Owing to this method, fracture surfaces, fiber-matrix interactions, and fiber structures formed in composites can be observed as a result of tests. In order to increase the surface conductivity of the samples, gold plating was made by using sputtering method. In order to see the hybridization effects, in addition to analyzing the quantitative data, the effects of mechanical fracture in macroscopic way can be

examined by SEM. Morphological analysis was conducted at CUMERLAB (Cukurova University Central Research Laboratory).



Figure 3.19. Scanning electron microscope

3.2.3.4. Loss on Ignition Test Analysis

One of the main parameters in specifying the mechanical characteristics of composites is the fiber volume ratio. The fiber volume fraction can be experimentally determined by the ignition loss method or the matrix burn-off test (ASTM D 2584). Matrix burn tests were performed at Automotive Engineering Laboratory of Cukurova University according to ASTM D2584-02 Standard Test Method for Ignition Loss of Cured Reinforced Resins to determine the ignition loss of cured reinforced resins. In this method, a composite sample is heated in a porcelain crucible until the epoxy matrix ignites in an electric muffle furnace that reaches 350°C (Figure 3.20). Although the standard method recommends a furnace temperature of 565 °C, this furnace temperature is sufficient for carbon, aramid,

and basalt fiber extraction (Karaçor, 2020). The resin part of the composite sample is separated from the fiber part in a hot furnace environment. The residue is filtered and weighed.

The ignition loss of the specimens is calculated according to the ASTM D 2584 standard as follows:

$$IL = \left[\frac{W_1 - W_2}{W_1} \right] \times 100$$

where IL is the ignition loss (%), W_1 is the measured weight of the sample before the testing (g) and W_2 is the measured weight of the sample (residue) after the testing (g).



Figure 3.20. Electric muffle furnace

3.2.3.5. Water Absorption Analysis

The purpose of this analysis is to determine the capacity of manufactured materials to absorb water in normal water by considering ASTM D 5229 standards. Composite samples were saturated with water from the surface during their stay in the container.

Water absorption test was conducted at Automotive Engineering Laboratory of Cukurova University. Five different composite samples, C9, A3B6, A5B4, B4A5 and B6A3 produced according to ASTM standard were prepared. First, the dry weights of five different products were measured on a digital scale, after which the samples were immersed to water for a certain period. The amount of water absorbed by the samples was weighed at regular intervals and was noted periodically. The test was carried out at room temperature, tap water was used in the containers in which the samples were placed.

The amount of water absorption was calculated by the formula (3.2).

$$M = (W_i - W_d) / (W_d) \times 100 \quad (3.2)$$

W_i = Weight Water Absorbed

W_d = Weight Dry material

The water absorption test of the materials produced was shown in Figure 3.21.



Figure 3.21. Water absorption of test samples; a) B5A4, b) B6A3, c) A3B6, d) C9, e) A5B4

3.2.3.6. Hardness Test Analysis

In materials science, hardness is defined as the materials represent the capacity to resist permanent deformations proportional to the bond strength of their atoms. The Rockwell hardness test is the most frequently used hardness testing method and is considered to be more accurate and easier to perform than other hardness tests. This test can be performed on all metals and composites unless the size, shape, or surface conditions of the specimens are prohibitive. The hardness measurement based on the net increase in depth of impression as a load is applied and is measured according to the ASTM D 785 standard. In this test, a standard specimen of dimension at least 6.4 mm in thickness is placed on the surface of the Rockwell hardness tester a minor load (10 kgf) is applied. Then, the major load (150 kgf) is applied to specimen for a specified time which depends on the chosen

scale (Saba et al., 2018). Hardness test was conducted at Mechanical Engineering Laboratory of The Faculty of Ceyhan Engineering of Cukurova University.



Figure 3.22. Hardness test machine

The hardness test was performed by the machine, which test loads ranging from 10 kgf to 150 kgf, to estimate the degree of material's abrasion to cut, scratch or indentation (Figure 3.22). In this test, Rockwell C scale was chosen to determine the hardness value of composite materials. While measuring, 10 values were obtained for the hardness of each sample, and the average of these values was recorded as the hardness value of the composite product.



4. RESULTS AND DISCUSSIONS

4.1. Tensile Test Analysis Results

After tensile test, a stress-strain graph of C9, B6A6, A6B6, B8A4 and A4B8 composite samples which is obtained from the software of tensile testing machine is shown in Figure 4.1, 4.2, 4.3, 4.4 and 4.5, respectively.

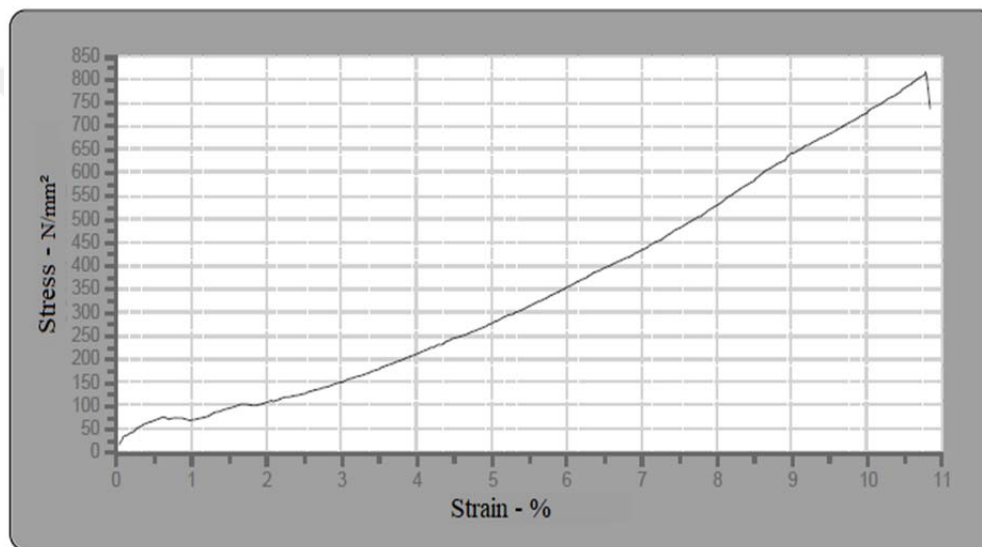


Figure 4.1. Stress-Strain graph of a C9 composite material

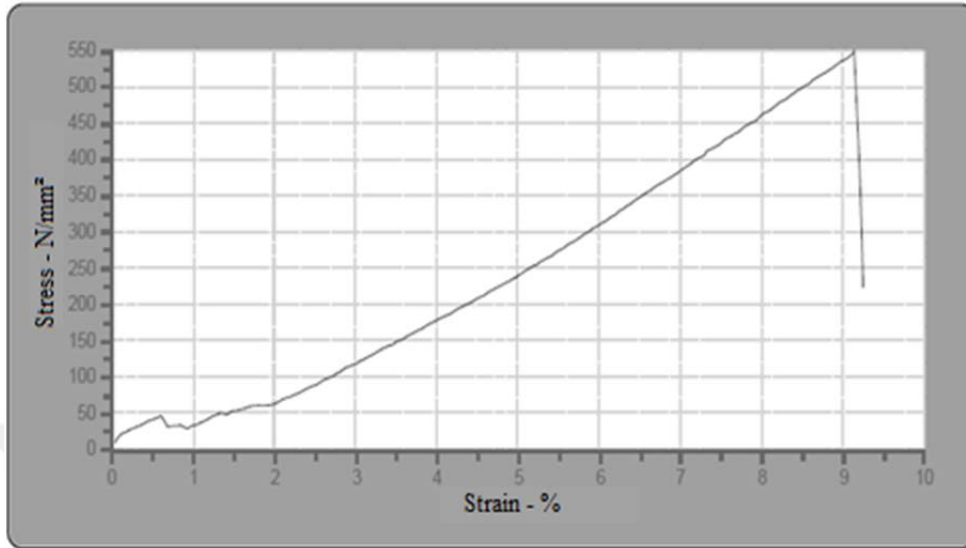


Figure 4.2. Stress-Strain graph of a B6A6 hybrid composite material

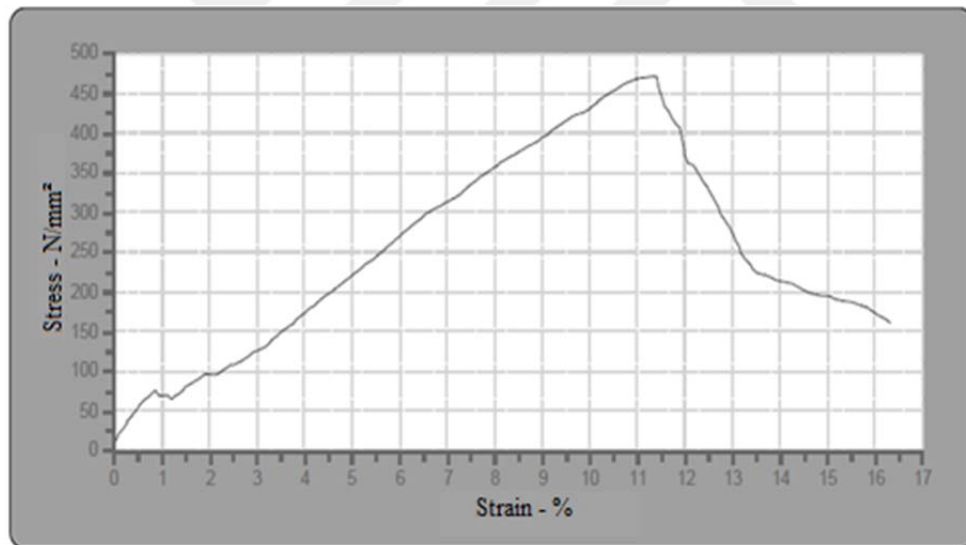


Figure 4.3. Stress-Strain graph of an A6B6 hybrid composite material

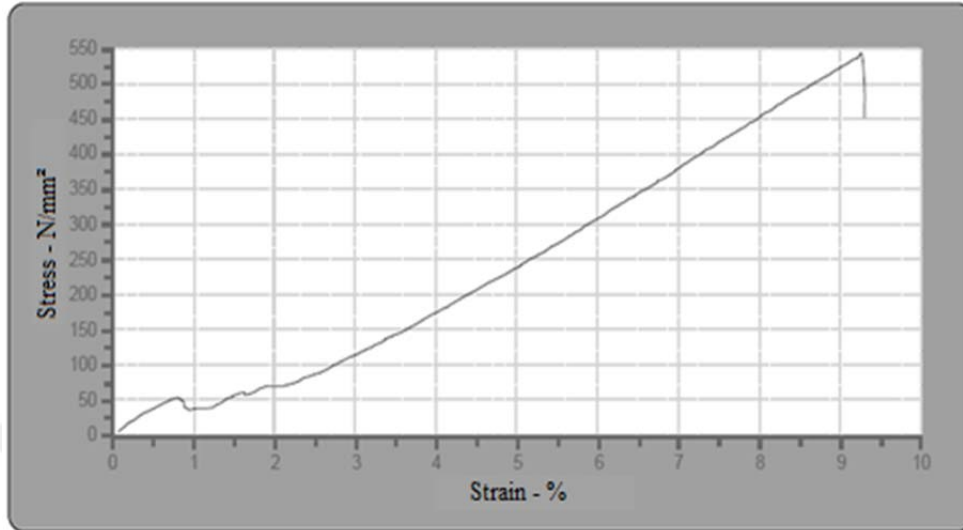


Figure 4.4. Stress-Strain graph of a B8A4 hybrid composite material

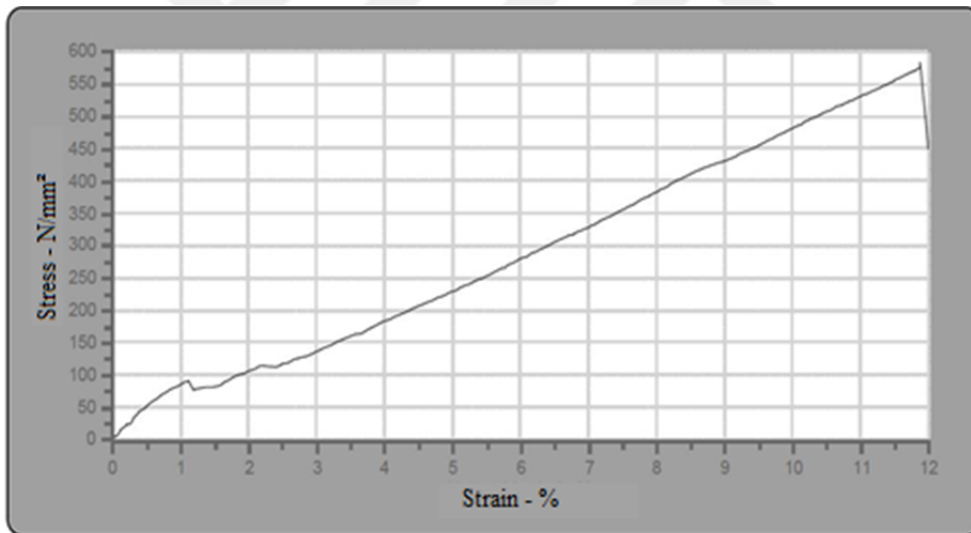


Figure 4.5. Stress-Strain graph of an A4B8 hybrid composite material

As it is stated in the standard method, five different samples for each composite sample were tested and the obtained results are shown in Table 4.1 with details, where E is elastic modulus (N/mm^2), ϵ is the elongation rate (%), F is the applied force (kN) and σ is the tensile strength (N/mm^2) of composite materials.

In Figure 4.6, one sample of each composite material after tensile test was shown.



Figure 4.6. Samples after Tensile test, left to right; C9, A6B6, B6A6, A4B8, B8A4

Table 4.1. Tensile test results

Composite Type	Composite Codes	E (N/mm ²)	ε (%)	F (kN)	σ (N/mm ²)
Carbon Fiber	C9-1	6756	14,1	44,4	893
	C9-2	7367	11,8	43,5	831
	C9-3	7089	22,1	44,8	900
	C9-4	7866	10,8	40,3	812
	C9-5	8054	11,2	40,8	826
Hybrid	A6B6-1	4249	16,3	24,9	472
	A6B6-2	3241	19,3	19,9	377
	A6B6-3	4059	19,9	24,4	464
	A6B6-4	4201	19,9	27,1	513
	A6B6-5	4559	11,9	28,9	564
Hybrid	B6A6-1	6907	9,5	30,1	572
	B6A6-2	6618	9,2	29,6	547
	B6A6-3	6632	9,5	30,8	570
	B6A6-4	6812	9,6	30,5	580
	B6A6-5	6737	9,9	30,9	589
Hybrid	A4B8-1	4312	11,9	25,2	534
	A4B8-2	4672	12	25,6	575
	A4B8-3	4199	12,2	24,9	529
	A4B8-4	4527	11,2	25	531
	A4B8-5	4372	12,1	26,3	555
Hybrid	B8A4-1	5378	9,1	24,2	509
	B8A4-2	6095	9,4	26,8	564
	B8A4-3	6299	8,7	23,3	505
	B8A4-4	6568	9,3	24,9	540
	B8A4-5	5810	8,8	23,3	481

The average tensile strength results of five different specimens are presented in Figure 4.7. According to the results, homogeneous carbon fiber composite sample, which is C9, has the highest tensile strength among all the produced samples. B6A6 hybrid sample has higher tensile strength compared to other hybrid samples. However, A6B6 specimen showed the lowest tensile strength compared to other specimens despite having the same fiber ratio with B6A6 hybrid sample. In this scenario, A6B6 hybrid sample had 16,5% less tensile strength value than B6A6 hybrid sample and this result could be explained with fiber stacking sequence difference between these specimens. The tensile strength of A4B8 specimen was 4,6% higher than B8A4 specimen which has the same fiber ratio but different stacking order. It is also seen that using aramid fibers at the outer layers in A4B8 hybrid composite sample showed positive effect on tensile strength, while using basalt fibers at the outer layers in B6A6 hybrid specimen showed positive effect on tensile strength.

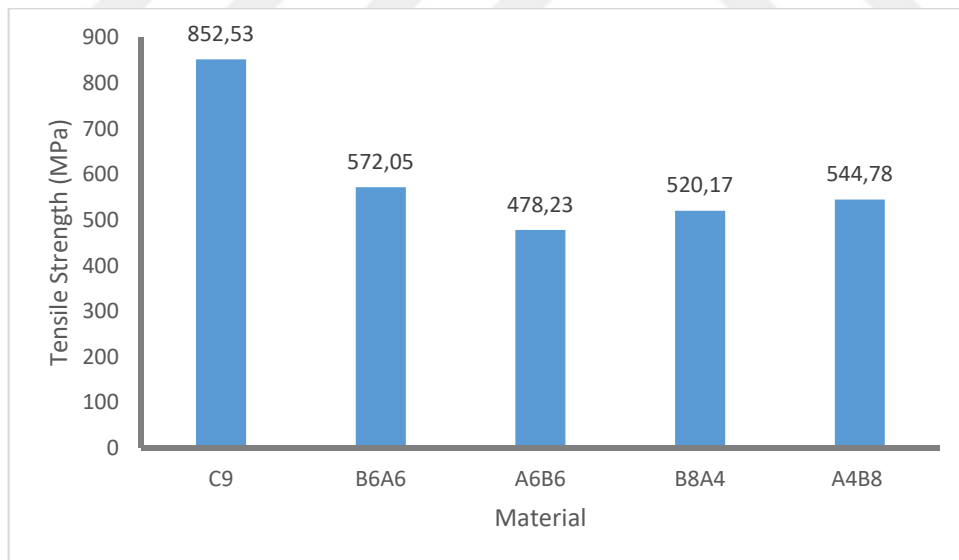


Figure 4.7. Average tensile strength of composite materials

In Figure 4.8, the average elongation rate of composite materials is shown. It is observed from these result that A6B6 hybrid sample has the highest elongation rate and B8A4 specimen has the lowest one among others. It is also seen that C9 and A4B8 samples have the elongation rate of 14% and 11,88%, respectively.

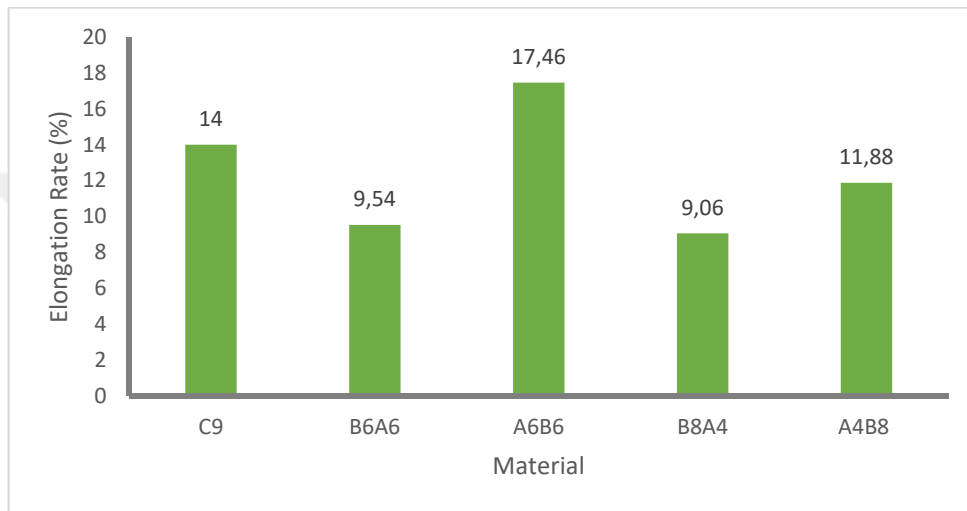


Figure 4.8. Average elongation rate of composite materials

An elastic modulus is a measurement of a material's resistance to elastic deformation when a stress is applied to the material. The elastic modulus can be defined as a slope of the stress-strain curve of the material in the elastic deformation region. A higher elastic modulus is the indication of a stiffer material (Askeland and Fulay, 2006). When the average elastic modulus of tensile test specimens is examined in Figure 4.9, it is seen that C9 sample has a 10% higher elastic modulus value than B6A6 sample. It can be seen that changing the fiber sequence of B6A6 sample has significantly affected the elastic modulus which A6B6 specimen has a 40% less elastic modulus value than B6A6. Moreover, the same situation can be seen between B8A4 and A4B8 hybrid composite samples. A4B8 specimen has a 27% less elastic modulus value than B8A4 specimen.

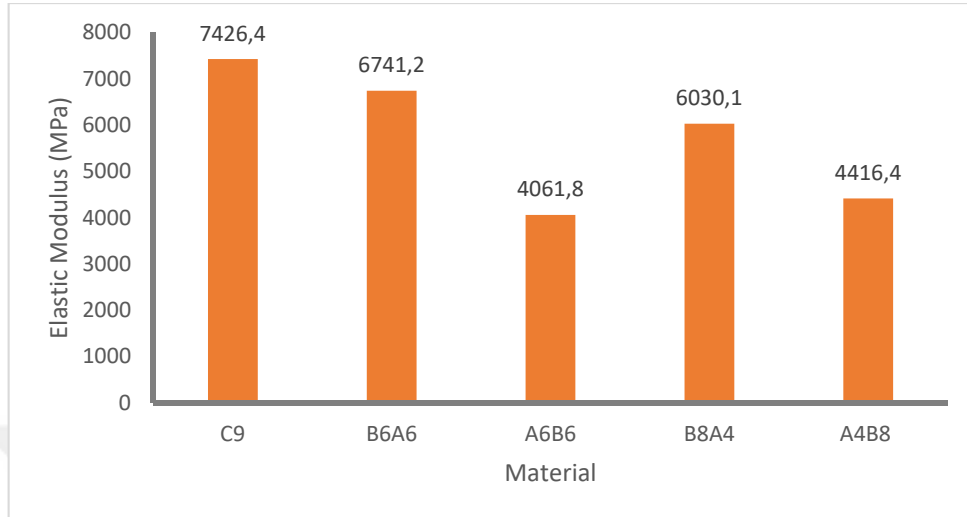


Figure 4.9. Average elastic modulus of composite materials

4.2. Impact Test Analysis Results

The impact energy of the composite samples absorbed were tabulated in Figure 4.10. The results have revealed that B24A24 hybrid composite has the highest impact energy (67,34 J). C44 has the lowest impact energy (20,41 J) due to carbon fiber is a highly brittle material. From this chart, it is visible that hybrid composites consist of more aramid fiber have higher impact energies and the increase in the basalt fiber ratio decreased the amount of absorbed energy. This result can be explained by having high impact resistance of aramid fiber and brittle characteristic of basalt fiber. On the other hand, B32A17 and A17B32 hybrid samples have similar impact energy values since they have the same fiber ratio. When the effect of the stacking order was examined, it was seen that A24B24 had 21% less impact energy than B24A24 on average, while A17B32 had 7% less than B32A17 laminated composites.

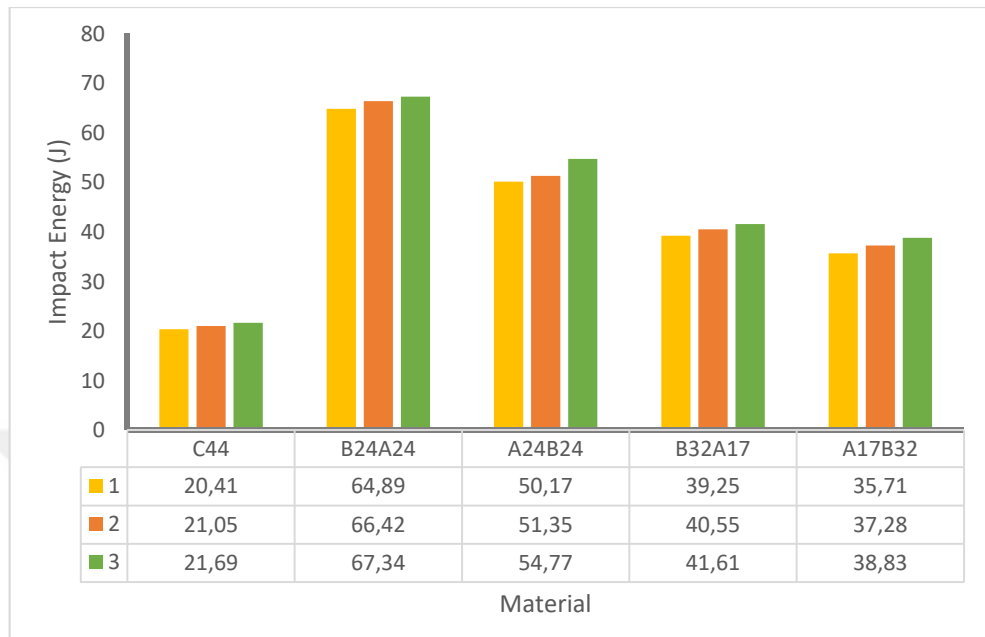


Figure 4.10. Impact energy values of produced composite samples

In Figure 4.11, the impact strength graph was presented, and it was seen that B24A24 hybrid composite had the highest impact strength value among other materials. On the other hand, C44 specimen which produced with pure carbon fiber had the lowest value in terms of impact strength. A24B24 specimen has 21% less impact strength than B24A24 specimen with 5,21 kJ/mm and the impact strength of A17B32 hybrid sample is 16% less than B32A17 hybrid sample with 3,72 kJ/mm. The materials after the impact test are demonstrated in Figure 4.12.

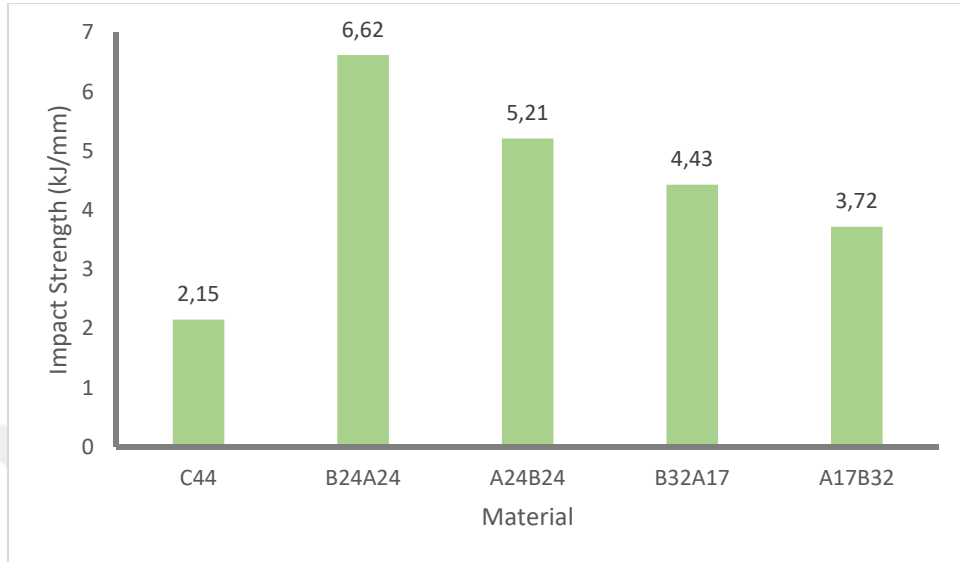


Figure 4.11. Impact strength of composite samples produced



Figure 4.12. Samples after Charpy impact test, from left to right; C44, B24A24, A24B24, B32A17, A17B32

4.3. Morphological Analysis Results

The SEM images were obtained to examine the morphologies of composite materials after the tensile test. Figure 4.13 and 4.14 demonstrate the SEM images of C9 composite structure. Through these images, it was observed that there is a strong bonding between carbon fiber and epoxy matrix. This strong bonding explains why C9 composites have the highest tensile strength. Also, there is less fiber breakage compared to hybrid composite structures. The structure of B8A4 hybrid composite is shown in Figure 4.15 and 4.16. In these figures, extensive fiber-matrix debonding and delamination were observed. There are more fiber breakage and gaps in the structure of B8A4 compared to C9 composite material. In addition, fiber shrinkage and fiber splitting can be seen in Figure 16. This indicates the fact that natural fibers have different chemical bonding characteristics than synthetic fibers and they do not form a good bond with the matrix (Ozkur et al., 2021). In this case, one of the reasons of B8A4 sample having significantly less tensile strength than C9 sample can be expressed by bonding characteristics of fibers.

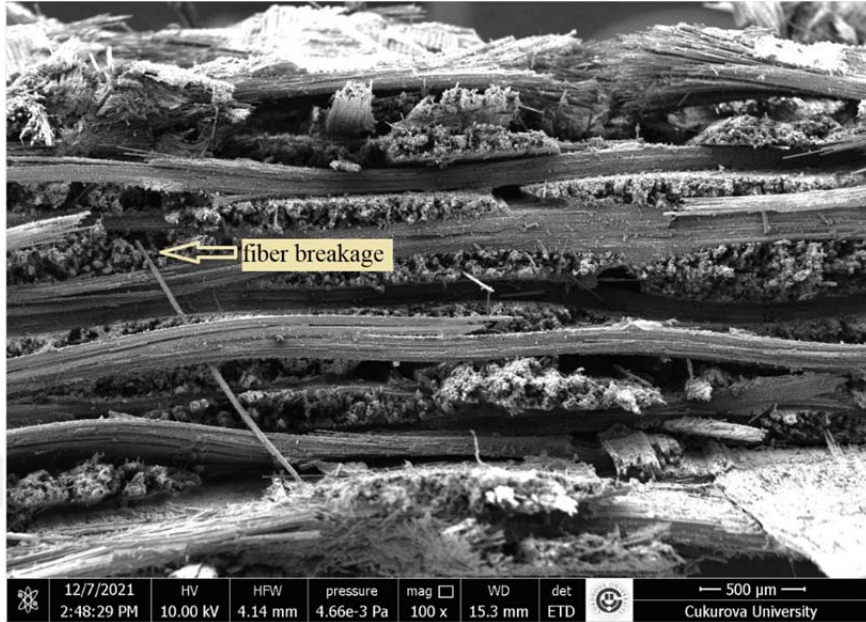


Figure 4.13. SEM image of C9 sample after tensile test (X100)

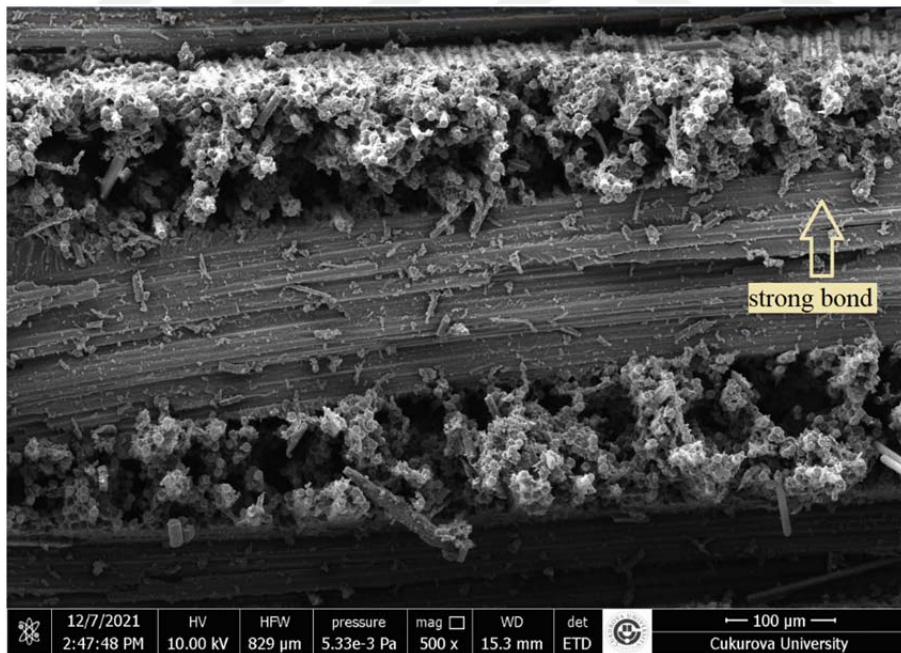


Figure 4.14. SEM image of C9 sample after tensile test (X500)

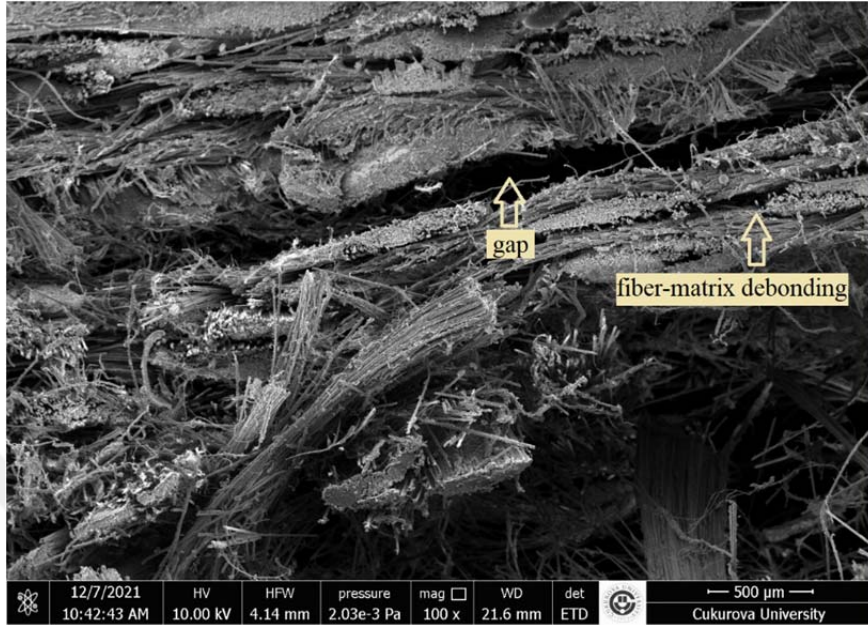


Figure 4.15. SEM image of B8A4 sample after tensile test (X100)

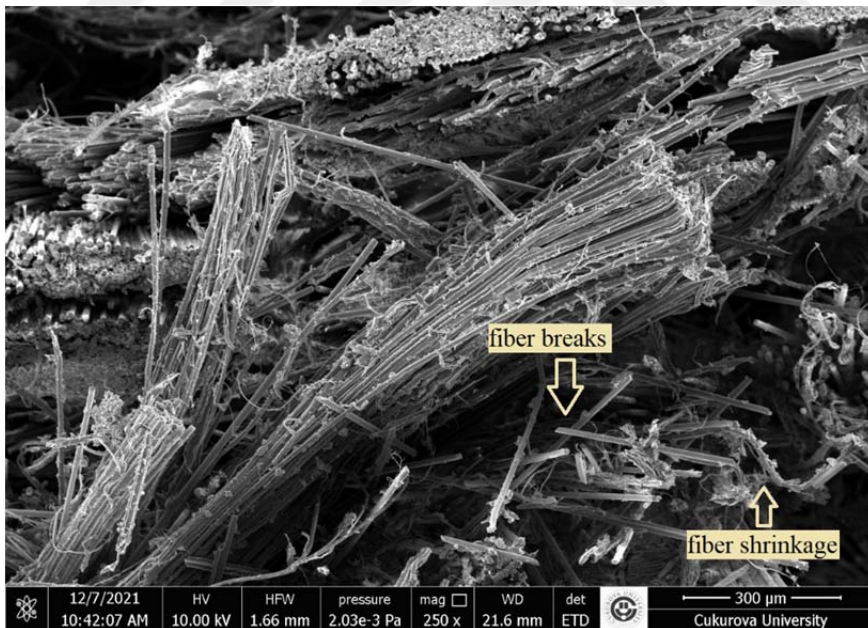


Figure 4.16. SEM image of B8A4 sample after tensile test (X500)

In Figure 4.17 and 4.18, the structure of A4B8 hybrid composite material is presented. A weak bonding between the matrix and fibers compared to other composite samples is seen in Figure 17. In addition, extensive fiber splitting and larger gaps compared to other samples can be seen in Figure 4.17 and 4.18. On the other hand, the structure of B6A6 hybrid sample is shown in Figure 4.19 and 4.20. Through these images, the bonding between the matrix and fibers in B6A6 specimen was stronger than A4B8 specimen. When Figure 4.19 was examined, there were fewer gaps in comparison to A4B8 hybrid sample. The structure of A6B6 hybrid sample is demonstrated in Figure 4.21 and 4.22. In these figures, it is visible that there is fiber breakage, extensive fiber-matrix debonding and delamination in the structure. In addition, there are more gaps in A6B6 sample compared to B6A6 sample as it is seen in Figure 4.21 and 4.19. These findings explain the reason of A6B6 hybrid composites having lower average tensile strength value than B6A6 hybrid composites.

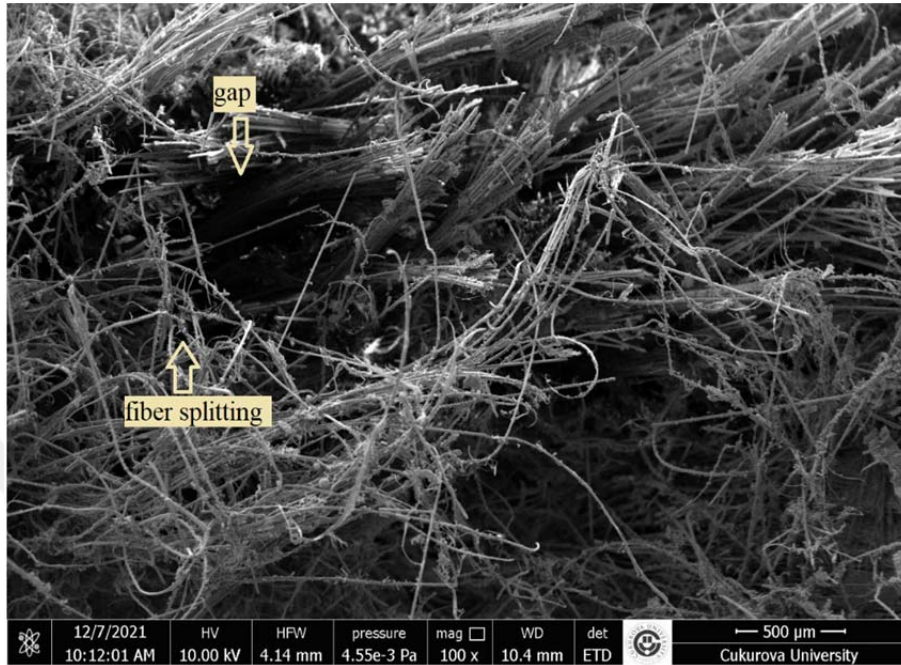


Figure 4.17. SEM image of A4B8 sample after tensile test (X100)

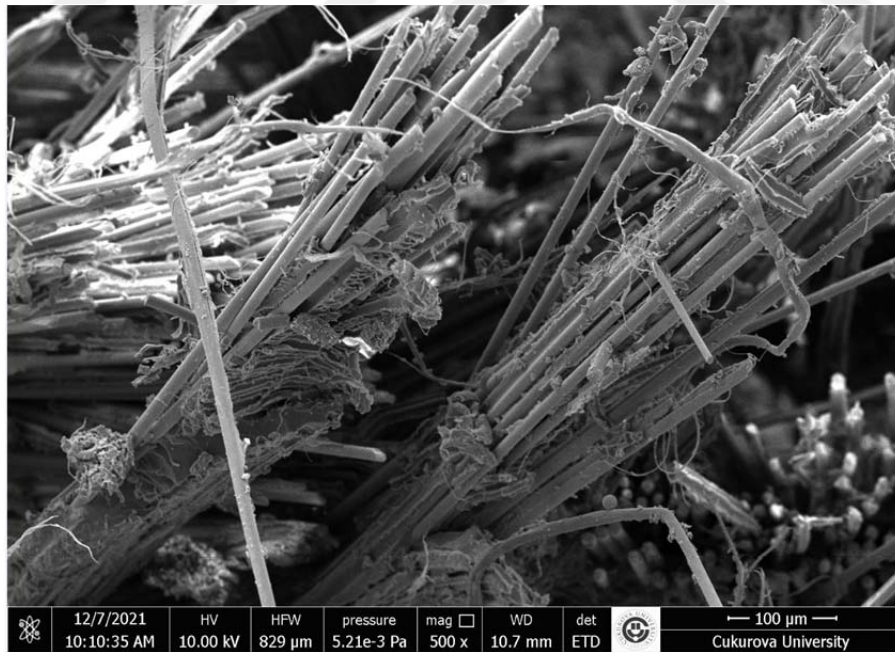


Figure 4.18. SEM image of A4B8 sample after tensile test (X500)

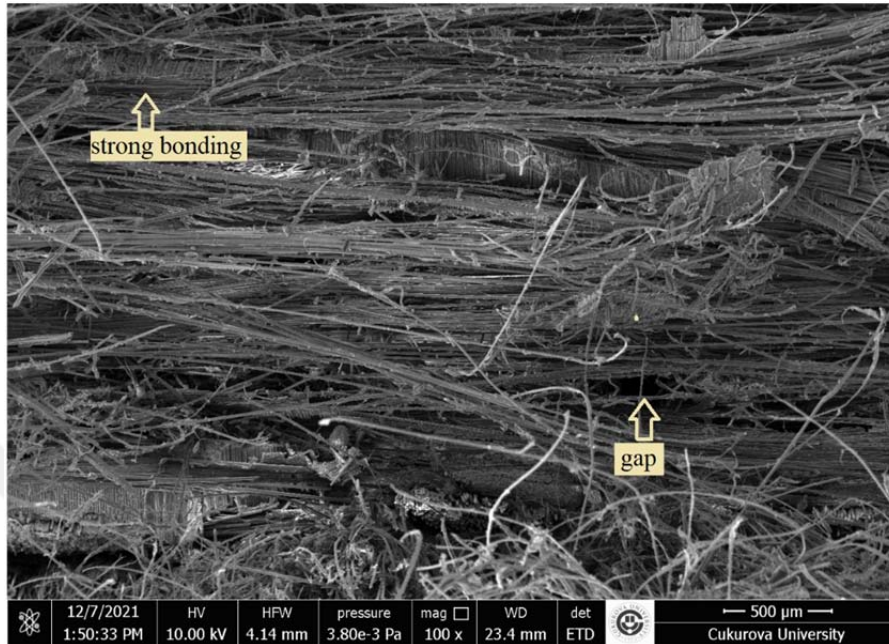


Figure 4.19. SEM image of B6A6 sample after tensile test (X100)



Figure 4.20. SEM image of B6A6 sample after tensile test (X500)

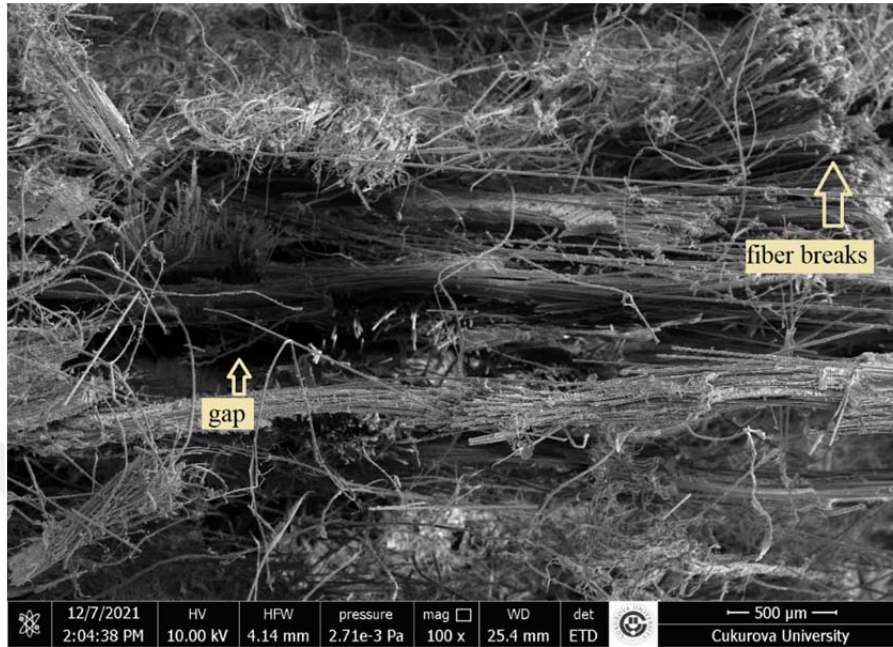


Figure 4.21. SEM image of A6B6 sample after tensile test (X100)

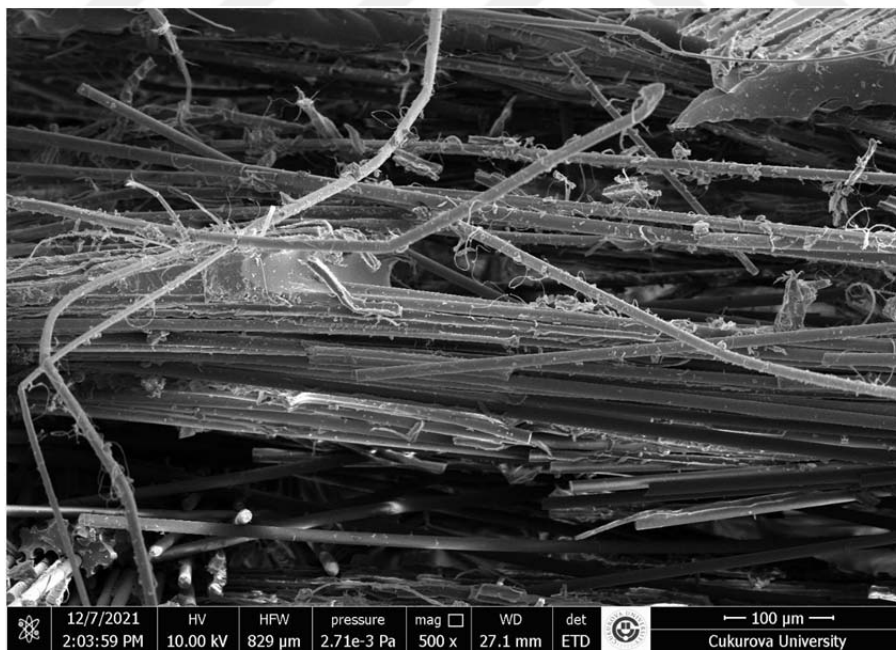


Figure 4.22. SEM image of A6B6 sample after tensile test (X500)

After Charpy impact test, the SEM images of test samples were also obtained to examine the structure of produced composite materials. The structure of C44 sample is shown in Figure 4.23. Despite a strong bonding exists between carbon fiber and epoxy matrix, a delamination in the matrix was observed in the structure of C44 sample. The reason of C44 having the lowest impact energy can be expressed by the brittle nature of carbon fiber which absorbs energy by cracking (Romo et al., 2017). The bonding between the matrix material and reinforcement materials in hybrid composites is not as strong as in C44 due to different bonding characteristics of fibers, as mentioned before. In Figure 4.24 and 4.25, small gaps fiber separations were detected in the structure of B32A17 and A17B32 hybrid composite materials. On the other hand, when the structure of B24A24 hybrid sample was examined, a large gap can be seen in Figure 4.26 in addition to fiber shrinkage. Fiber breakage and fiber splitting were observed in the structure of A24B24 hybrid sample shown in Figure 4.27.

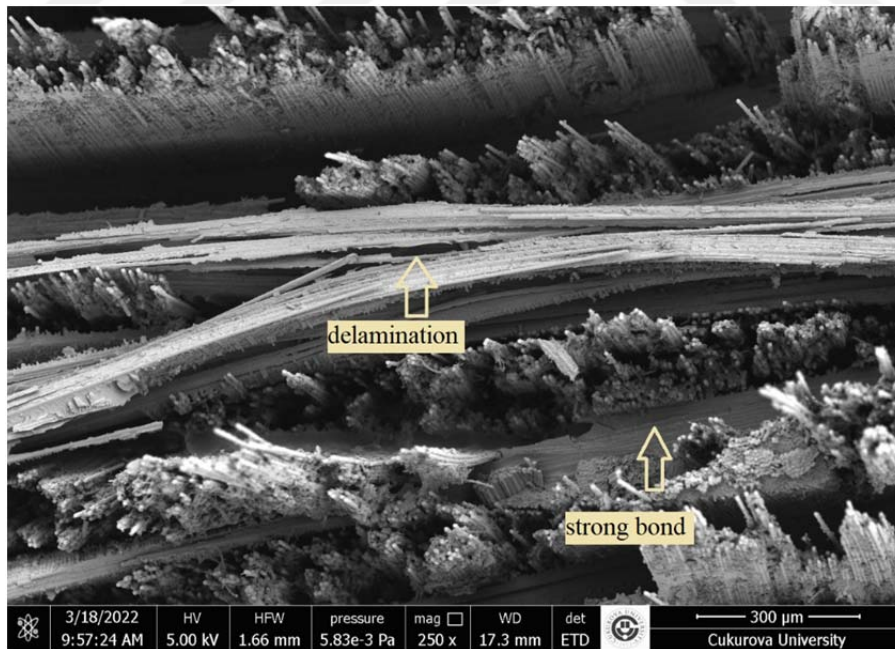


Figure 4.23. SEM image of C44 sample after impact test (X250)

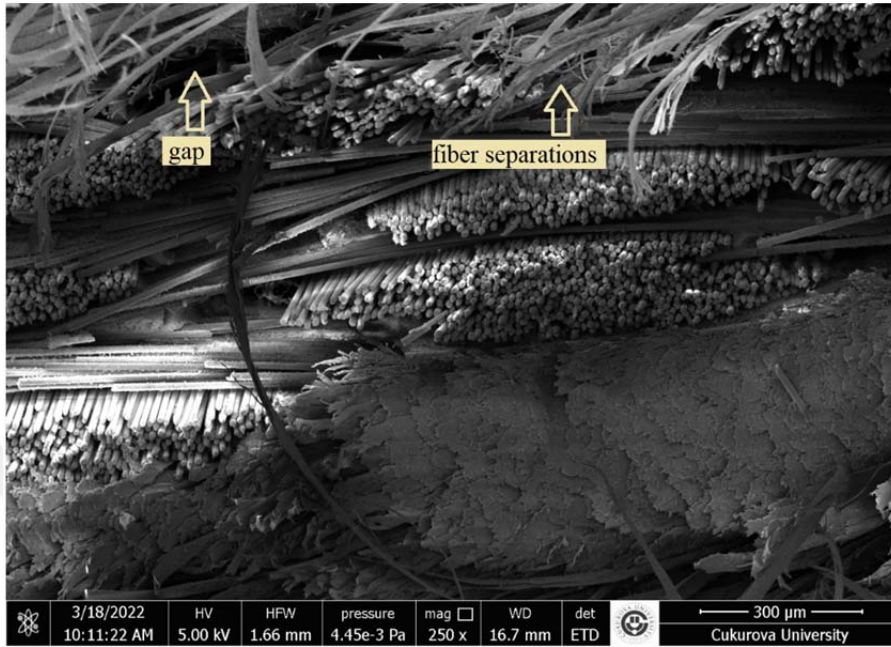


Figure 4.24. SEM image of B32A17 sample after impact test (X250)



Figure 4.25. SEM image of A17B32 sample after impact test (X250)

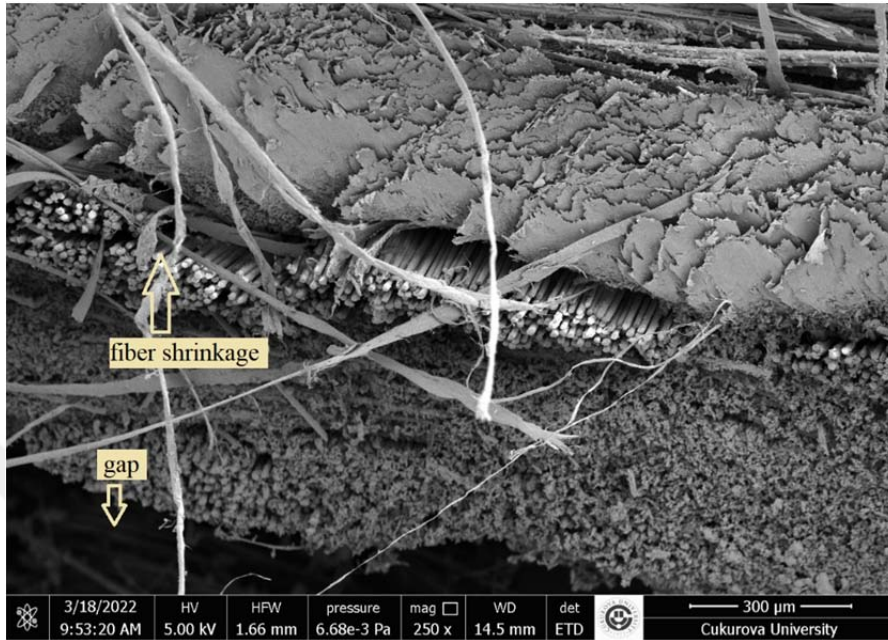


Figure 4.26. SEM image of B24A24 sample after impact test (X250)

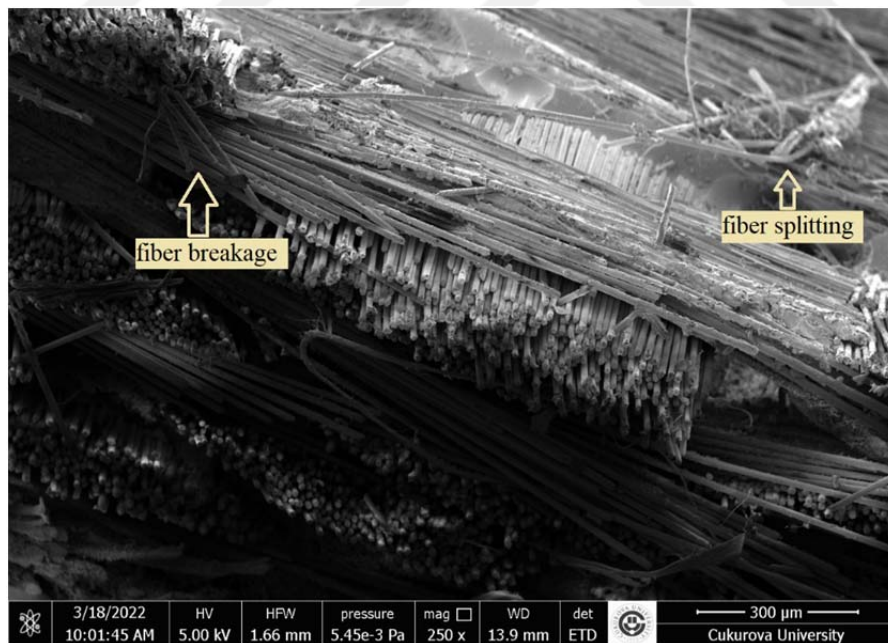


Figure 4.27. SEM image of A24B24 sample after impact test (X250)

4.4. Loss on Ignition Test Analysis Results

As it is mentioned in the standard method, three tests were conducted for the composite samples and the average weights of specimens are demonstrated in Table 4.2. In this test, the results have shown that B4A3 hybrid composite sample has the highest ignition loss value as a percent by weight of the sample. A3B4 and B3A4 hybrid specimens have similar ignition loss values despite having different fiber contents. Moreover, the increase in aramid fiber ratio has decreased the ignition loss by weight of the B3A4 and A4B3 hybrid composite samples as it can be seen from the table. In addition, C7 composite samples have very close results to B3A4 hybrid composite materials. The temperature was one of the most important parameters in this test. During this analysis, it was observed that when the temperature is exceeded 350°C, epoxy resin is burned. Therefore, the correct results could not be obtained over 350°C (Karaçor, 2020). The average required time for this combustion was approximately 3 minutes.

Table 4.2. Ignition loss test results of composite samples

Samples	Arithmetic Average of W_1 Weights (g)	Arithmetic Average of W_2 Weights (g)	Ignition loss, weight (%)
C7	9,7193	9,5551	1,69
B4A3	9,2384	9,0479	2,06
A3B4	9,4816	9,3091	1,82
B3A4	9,8186	9,6435	1,78
A4B3	9,4921	9,3456	1,54

4.5. Water Absorption Analysis Results

In order to determine the water absorption amount of the materials, first, the materials were dipped the containers filled with water, and then pulled out after 168 hours of observation. During this time, weight changes were calculated. After 168 hours of data collection, the available values of C9, A3B6, B4A5, B6A3 and A5B4 composite samples are shown in Figure 4.28, 4.29, 4.30, 4.31 and 4.32, respectively. These figures demonstrate the water absorption amount of produced specimens approximately.

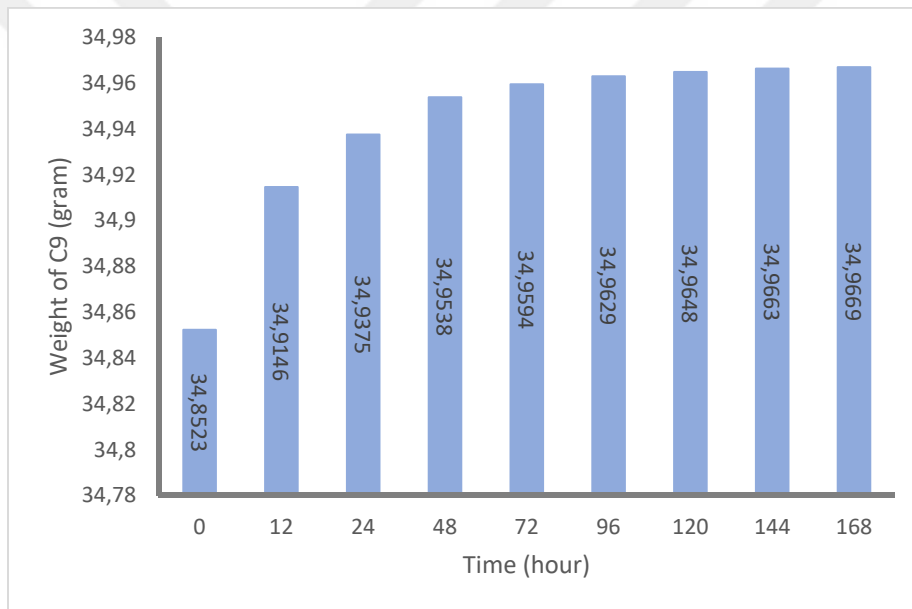


Figure 4.28. Water absorption of C9 composite material

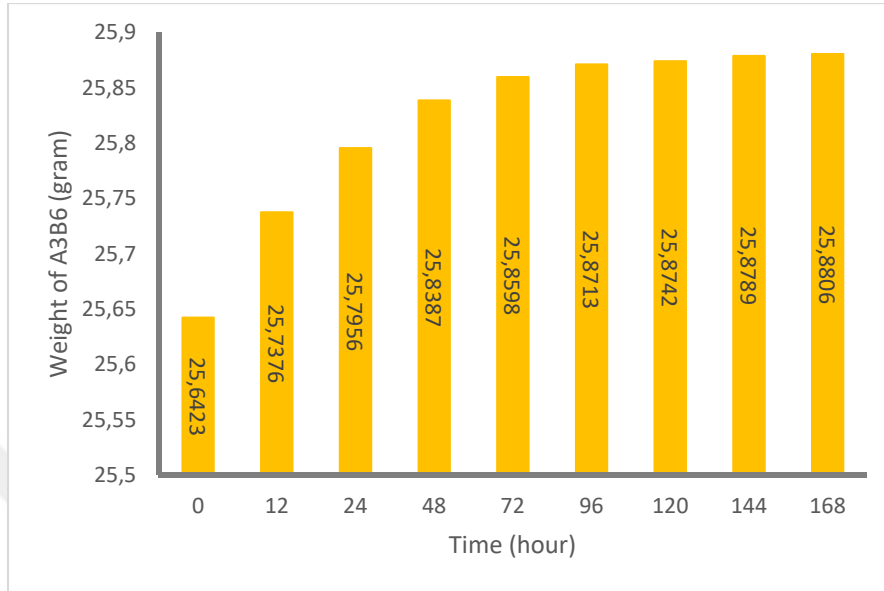


Figure 4.29. Water absorption of A3B6 hybrid material

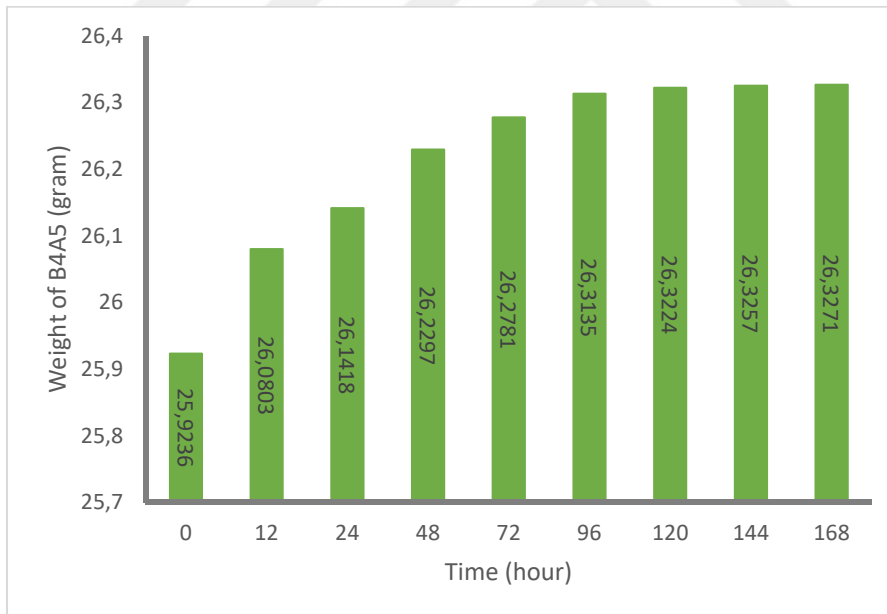


Figure 4.30. Water absorption of B4A5 hybrid material

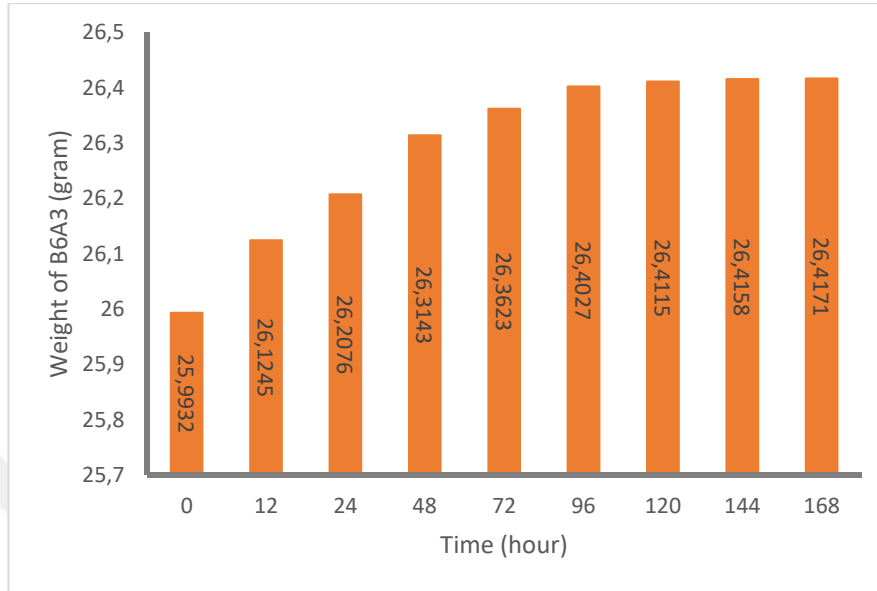


Figure 4.31. Water absorption of B6A3 hybrid material

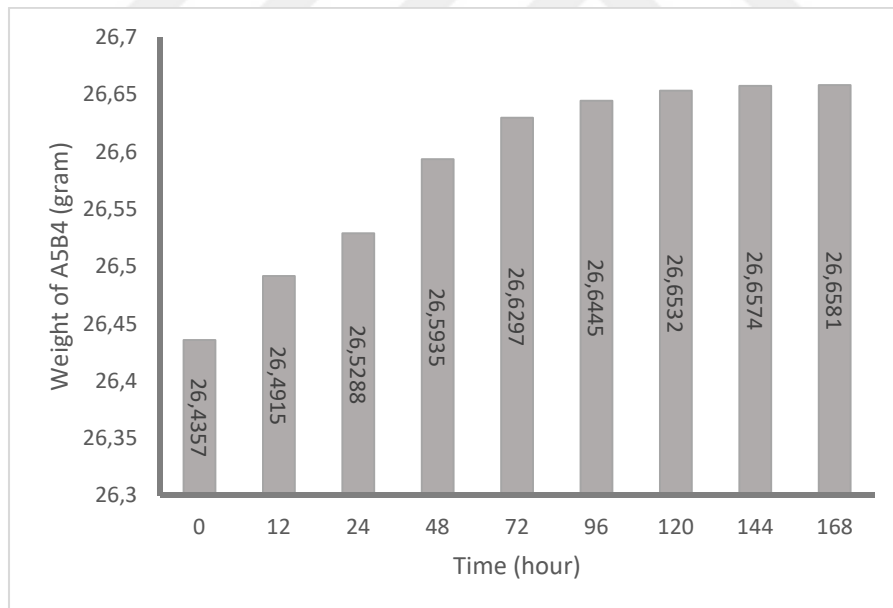


Figure 4.32. Water absorption of A5B4 hybrid material

Periodic measurements have revealed that C9 has the lowest absorption rate of 0,34% among all composites. A5B4 is the closest to C9 with 0,84% of water absorption and B4A5 has 1,56% water absorption rate. The amount of water A3B6 absorbed is 0,93% of its weight, and B6A3 has the highest absorption rate of 1,64% compared other samples. The results have shown that the water absorption amount of the hybrid composite materials changed substantially with different stacking order. In addition, when the basalt fiber content in hybrid composites is increased, it can be clearly seen that the water absorption amount of these materials is also increased. These results can be attributed poor moisture resistance of natural fibers including basalt fiber (Tajuddin et al., 2016). It should be considered that there are many factors affecting the water absorption amount of hybrid composites other than stacking order and fiber content, such as humidity, temperature, voids/defects, and thickness effects.

4.6. Hardness Test Analysis Results

The hardness value of the produced composites was shown in Figure 4.33. After examination of Rockwell hardness test results, it is seen that C44 specimen has the highest hardness value and B32A17 specimen has the lowest hardness value among all the produced composites. As it is seen from the graphic, A24B24 specimen has 1.4 times higher hardness value than B24A24 specimen, while the hardness value of A17B32 hybrid sample is 1.56 times higher than B32A17 hybrid sample. Through these results, it was found that hybrid samples that consist of aramid fibers at the outer layers, which are A24B24 and A17B32, showed consistently better performance than the ones which consist of basalt fibers at the outer layers. These results can be explained by high stiffness and damage resistance of aramid fiber (Prashanth et al., 2017). Mounika et al. (2021) also presented similar hardness values of aramid fiber reinforced composites in a study.

The obtained results from this test showed that fiber stacking order could significantly affect the performance of composite materials in terms of hardness.

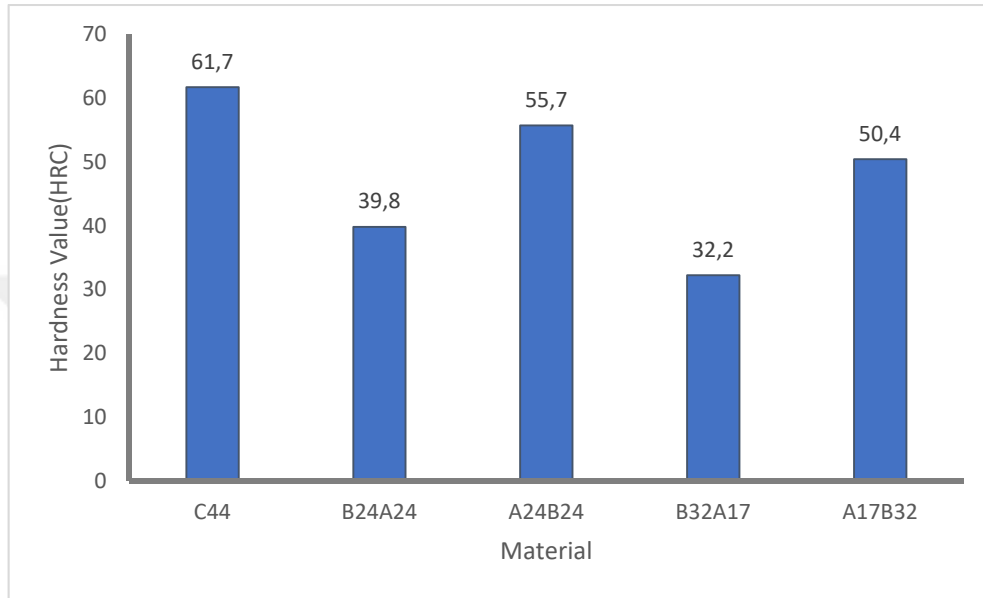


Figure 4.33. Hardness values of composite materials

5. CONCLUSIONS

In the scope of this study, various natural fiber reinforced hybrid composite samples as an alternative to carbon fiber composites have been designed, produced and tested. Hybrid composite samples manufactured with different fiber ratios and stacking sequences using basalt fiber and aramid fiber. Tensile test, hardness test, water absorption test, loss on ignition test, impact test, and Scanning Electron Microscopy (SEM) analysis were conducted in order to determine the mechanical properties of these fabricated products and the obtained results during this study can be summarized as the following;

- The results of tensile test showed that C9 specimens had the highest tensile strength among other produced composite materials. In hybrid composite samples, B6A6 specimen had higher tensile strength than other hybrid composite samples.
- It was also observed from tensile test results that A6B6 hybrid sample had 16,5% less tensile strength value than B6A6 hybrid sample, while the tensile strength value of A4B8 specimen was 4,6% higher than B8A4 specimen.
- According to Charpy impact test results, C44 sample had the lowest impact energy (20,41 J) as expected, due to brittle nature of carbon fiber. B24A24 hybrid sample, on the other hand, had the highest impact energy value (67,34 J) among all the composites. A24B24 had 21% less impact energy than B24A24. In addition, the average impact energy value of B32A17 specimen was 7% higher than A17B32 specimen.
- Also, when the impact strengths of composites were examined, it was found that the impact strength of B24A24 hybrid sample was 3 times higher than C44 specimen.

- Morphological analysis results demonstrated that there was a strong bonding between carbon fiber and epoxy matrix which is seen in the SEM image of C9 sample. In the structures of B8A4 and A6B6 hybrid samples, extensive fiber-matrix debonding, delamination and gaps were observed.
- In addition, a weak bonding between the matrix and fibers in the structure of A4B8, fewer gaps in B6A6 hybrid samples were observed in addition to extensive fiber splitting in A4B8 sample.
- Also, delamination in C44 sample, small gaps in B32A17 and A17B32 hybrid composites, fiber shrinkage and fiber splitting in B24A24 specimen and fiber breakage in A24B24 specimen was observed through SEM images.
- Ignition loss results of composite materials revealed that B4A3 hybrid composite sample had the highest ignition loss value as a percent by weight of the sample (2,06%), while A4B3 had the lowest value (1,54%). It was also seen that the correct results could not be obtained over 350°C in this test. Because epoxy resin is burned when the temperature is exceeded 350°C.
- According to water absorption test results, the water absorption amount of C9, B6A3, A3B6, A5B4 and B4A5 samples were determined as 0,34%, 1,64%, 0,93%, 0,84% and 1,56%, respectively. When these results were examined, it was found that increasing the ratio of basalt fiber increased the amount of water absorbed by the composites.
- The hardness test results demonstrated that pure carbon fiber composite sample, C44, had the highest hardness value with 61,7 HRC in all the samples produced.
- While the hybrid composite samples A24B24, B24A24, A17B32 and B32A17 had 55,7 HRC, 39,8 HRC, 50,4 HRC and 32,2 HRC, respectively. Through these results, it was seen that hybrid samples which consist of

aramid fibers at the outer layers had higher hardness value than the ones consist of basalt fibers.

- All these obtained results indicate that aramid fiber reinforced composite structures that are hybridized with basalt fiber reinforcement are adequate materials for use in exterior and interior parts of vehicles and also armored military vehicles. Due to the increasing requirement for novel materials which are environmentally friendly, renewable, bio-degradable and cost-effective, the natural fiber reinforced composites are considered as promising candidates in the automotive industry. In order to achieve the material with required specifications mentioned earlier, the hybridization of basalt fiber with another type of natural fibers rather than a synthetic fiber can be conducted in the future studies.



REFERENCES

- Advani, S. G., and Hsiao, K. T., 2012. Manufacturing techniques for polymer matrix composites (PMCs). Woodhead Publishing Limited.
- Agarwal, G., Patnaik, A., Sharma, R. K., and Agarwal, J., 2014. Effect of Stacking Sequence on Physical, Mechanical and Tribological Properties of Glass-Carbon Hybrid Composites. *Friction*, 2(4):354–364.
- Al-Hajaj, Z., Sy, B. L., Bougherara, H., and Zdero, R., 2019. Impact Properties of a New Hybrid Composite Material Made from Woven Carbon Fibres plus Flax Fibres in an Epoxy Matrix. *Composite Structures*, 208(August 2018):346–356.
- Alarifi, I. M., 2021. Investigation into the Structural, Chemical and High Mechanical Reforms in B4C with Graphene Composite Material Substitution for Potential Shielding Frame Applications. *Molecules*, 26(7):1–17.
- Arusoğlu, T., 2019. Properties of Natural Fiber Reinforced Thermoset Polymer Hybrid Composite. MSc Thesis, Çukurova University.
- Ary Subagia, I. D. G., Kim, Y., Tijing, L. D., Kim, C. S., and Shon, H. K., 2014. Effect of Stacking Sequence on the Flexural Properties of Hybrid Composites Reinforced with Carbon and Basalt Fibers. *Composites Part B: Engineering*, 58:251–258.
- Ashraf, W., Nawab, Y., Umair, M., Shaker, K., and Karahan, M., 2017. Investigation of Mechanical Behavior of Woven/Knitted Hybrid Composites. *Journal of the Textile Institute*, 108(9):1510–1517.
- Ashter, S. A., 2014. Thermoforming of Single and Multilayer Laminates Thermoforming of Single and Multilayer Laminates. Elsevier Inc.
- Askeland, D., and Fulay, P., 2006. The Science and Engineering of Materials. Cengage Learning.

- ASTM Standards and Literature References for Composite Materials, 2000. ASTM D 2584-02, Standard Method for Ignition Loss of Cured Reinforced Resins. American Society for Testing and Material, Philadelphia, PA.
- ASTM Standards and Literature References for Composite Materials, 2004. ASTM D 6110, Standard Test Method for Determining the Charpy Impact Resistance of Notched Specimens of Plastics. ASTM International.
- ASTM Standards and Literature References for Composite Materials, 2017. ASTM D 3039 / D 3039M-17, Standard Test Method for Tensile Properties of Polymer Matrix Composite Materials. ASTM International.
- ASTM Standards and Literature References for Composite Materials, 2015. ASTM D 785, Standard Test Method for Rockwell Hardness of Plastics and Electrical Insulating Materials. ASTM International.
- ASTM Standards and Literature References for Composite Materials, 2020. ASTM D 5229, Standard Test Method for Moisture Absorption Properties and Equilibrium Conditioning of Polymer Matrix Composite Materials. ASTM International.
- Bandaru, A. K., Patel, S., Sachan, Y., Alagirusamy, R., Bhatnagar, N., and Ahmad, S., 2016. Low Velocity Impact Response of 3D Angle-Interlock Kevlar/Basalt Reinforced Polypropylene Composites. *Materials and Design*, 105:323–332.
- Bolton, W., 1993. *Engineering Materials Technology* Second Edition. Newnes.
- Callister, W. D., 2007. *Materials Science and Engineering An Introduction* Journal of Materials Science (7 th). John Wiley & Sons Inc..
- Campbell, F. C., 2010. *Structural Composite Materials* Geostatistics. ASM International.
- Carolin, A., 2003. *Carbon Fibre Reinforced Polymers for Strengthening of Structural Elements*. PhD Thesis, Lulea University of Technology.
- Chand, S., 2000. Carbon Fibers for Composites. *Journal of Materials Science*, 35(6):1303–1313.

- Chauhan, V., Kärki, T., and Varis, J., 2019. Review of Natural Fiber-Reinforced Engineering Plastic Composites, Their Applications in the Transportation Sector and Processing Techniques. *Journal of Thermoplastic Composite Materials*, 35(8):1169-1209.
- Colombo, C., Vergani, L., and Burman, M., 2012. Static and Fatigue Characterisation of New Basalt Fibre Reinforced Composites. *Composite Structures*, 94(3):1165–1174.
- Cui, Y., Chang, J. M., and Wang, W. L., 2016. Fabrication of Glass Fiber Reinforced Composites Based on Bio-Oil Phenol Formaldehyde Resin. *Materials*, 9(11).
- Dehkordi, M. T., Nosratty, H., Shokrieh, M. M., Minak, G., and Ghelli, D., 2010. Low Velocity Impact Properties of Intra-Ply Hybrid Composites Based on Basalt and Nylon Woven Fabrics. *Materials and Design*, 31(8):3835–3844.
- EV-Volumes, 2020. EV Data Center 2020. Retrieved from <http://www.ev-volumes.com/datacenter/>
- Fiore, V., Scalici, T., Calabrese, L., Valenza, A., and Proverbio, E., 2016. Effect of External Basalt Layers on Durability Behaviour of Flax Reinforced Composites. *Composites Part B: Engineering*, 84:258–265.
- Flynn, J., Amiri, A., and Ulven, C., 2016. Hybridized Carbon and Flax Fiber Composites for Tailored Performance. *Materials and Design*, 102:21–29.
- Groover, M., 2010. *Fundamentals of Modern Manufacturing Materials, Processes and Systems* John Wiley & Sons.
- Hall, W., and Javanbakht, Z., 2021. *Design and Manufacture of Fibre Reinforced Composites*. Springer.
- Jawaid, M., and Abdul Khalil, H. P. S., 2011. Cellulosic/Synthetic Fibre-Reinforced Polymer Hybrid Composites: A Review. *Carbohydrate Polymers*, 86(1):1–18.
- Ji, J., 2015. *Lightweight Design of Vehicle Side Door*. PhD Thesis, Politecnico Di Torino.

- Karaçor, B., 2020. The Usage of Natural Fiber Reinforced Hybrid Composite Materials As An Alternative to Automobile Interior Plastics. MSc Thesis, Çukurova University.
- Karaçor, B., and Özcanlı, M., 2021. Effect of Various Matrix Materials on Mechanical Properties of Basalt/Jute/Glass Fiber Reinforced Hybrid Composites. Cukurova University Journal of the Faculty of Engineering, 36(4):941–954.
- Kompozitshop, 2019. Epoxy and Hardener. Retrieved from <https://www.kompozitshop.com/epoksi-recine-ve-sertlestirici>
- Kompozitshop, 2020. Carbon, Aramid, and Basalt Fiber. Retrieved from <https://www.kompozitshop.com/karbon-fiber-elyaf-takviyeler-carbon?view=0&pg=2>
- Kompozitshop, 2022. Carbon, Aramid, Basalt, and Glass Fiber. Retrieved from <https://www.kompozitshop.com/karbon-fiber-elyaf-takviyeler-carbon?view=0&pg=2>
- Kongwat, S., Jaroenjittakam, S., Chaianan, S., Atchariyauthen, I., and Jongpradist, P., 2021. Design for Crash Safety of Electric Heavy Quadricycle Structure. IOP Conference Series: Materials Science and Engineering, 1137(1):012012.
- Koronis, G., Silva, A., and Fontul, M., 2013. Green Composites: A Review of Adequate Materials for Automotive Applications. Composites Part B: Engineering, 44(1):120–127.
- Kumar, A.M., Parameshwaran, R., Rajasekar, R., Moganapriya, C., and Manivannan, R., 2022. A Review on Drilling of Fiber-Reinforced Polymer Composites. Mechanics of Composite Materials, 58:97-112
- Lee, D. G., and Suh, N. P., 2006. Axiomatic Design and Fabrication of Composite Structures: Applications in Robots, Machine Tools, and Automobiles OXFORD University press.

- Liu, Q., Lin, Y., Zong, Z., Sun, G., and Li, Q., 2013. Lightweight Design of Carbon Twill Weave Fabric Composite Body Structure for Electric Vehicle. *Composite Structures*, 97:231–238.
- Lopresto, V., Leone, C., and De Iorio, I., 2011. Mechanical Characterisation of Basalt Fibre Reinforced Plastic. *Composites Part B: Engineering*, 42(4):717–723.
- Mangino, E., Carruthers, J., and Pitarresi, G., 2007. The Future Use of Structural Composite Materials in the Automotive Industry. *International Journal of Vehicle Design*, 44(3–4):211–232.
- Mayyas, A. T., Mayyas, A. R., and Omar, M., 2016. Sustainable Lightweight Vehicle Design: A Case Study in Eco-Material Selection for Body-In-White. *Lightweight Composite Structures in Transport: Design, Manufacturing, Analysis and Performance*. Elsevier Ltd.
- Militký, J., Mishra, R., and Jamshaid, H., 2018. Basalt fibers. *Handbook of Properties of Textile and Technical Fibres*. Elsevier.
- Mohammad, J., Thariq, M., and Saba, N., 2019. *Mechanical and Physical Testing of Biocomposites, Fibre-Reinforced Composites and Hybrid Composites*. Woodhead Publishing.
- Mounika, S., Boorla, R., Bolisetty, K. A., and Teja, S., 2021. Experimental Investigation on Mechanical Properties of Fabricating Composite Using Kevlar Fiber. *AIP Conference Proceedings*, 2317(February):1-8.
- Munawar, M. A., Khan, S. M., Gull, N., Shafiq, M., Islam, A., Zia, S., Sabir, A., Ghouri, A. S., Butt, M. T. Z., and Jamil, T., 2016. Fabrication and characterization of novel zirconia filled glass fiber reinforced polyester hybrid composites. *Journal of Applied Polymer Science*, 133(27).
- Naik, V., Kumar, M., and Kaup, V., 2022. A Review on Natural Fiber Composite Materials in Automotive Applications. *Engineered Science*, 18:1–10.

- Nandaragi, S. R., Reddy, B., and Narayana, K. B., 2018. Fabrication, testing and evaluation of mechanical properties of woven glass fibre composite material. *Materials Today-Proceedings*, 5(1): 2429-2434.
- Ngo, T.-D., 2020. *Introduction to Composite Materials. Composite and Nanocomposite Materials - From Knowledge to Industrial Applications*. Intechopen.
- Novitskii, A. G., and Efremov, M. V., 2013. Technological Aspects of the Suitability of Rocks from Different Deposits for the Production of Continuous Basalt Fiber. *Glass and Ceramics (English Translation of Steklo i Keramika)*, 69(11–12):409–412.
- OECD, 2002. *Strategies to Reduce Greenhouse Gas Emissions from Road Transport (Summary in Spanish)*.
- Ozkur, S., Leskovšek, M., Golja, B., Demsar A., Sezgin, H., and Yalçın Eniş, İ., 2021. Characterization of Thermo-mechanical and Morphological Properties of Jute Fabric Reinforced Epoxy/AESO Bio-composites. *Fibers and Polymers*, 22(12):3414-3424.
- Palle, R. R., Schuster, J., Shaik, Y. P., and Kazmi, M., 2022. Fabrication and Characterization of Glass Fiber with SiC Reinforced Polymer Composites. *Open Journal of Composite Materials*, 12(01):16–29.
- Pornwannachai, W., 2015. *Flame Retardant Natural Fibre Composites for High Performance Applications*. PhD Thesis, University of Bolton.
- Prashanth, S., Subbaya, K.M., Nithin, K., and Sachhidananda, S., 2017. Fiber Reinforced Composites - A Review. *Journal of Material Science & Engineering*, 06(03):1-6.
- Quanjin, M., Rejab, M. R. M., Zhang, B., and Kumar, N. M., 2019. Filament Winding Technique: SWOT Analysis and Applied Favorable Factors. *SCIREA Journal of Mechanical Engineering*, 3(1):1-25.

- Randjbaran, E., Zahari, R., Abdul Jalil, N. A., and Abang Abdul Majid, D. L., 2014. Hybrid Composite Laminates Reinforced with Kevlar/Carbon/Glass Woven Fabrics for Ballistic Impact Testing. *Scientific World Journal*, 2014:1-7.
- Romo, J., Cañibano, E., and Merino, J. C., 2017. Lightweighting and passive safety for urban electric vehicle. *Electric Vehicles International Conference and Show*.
- Saba, N., Jawaid, M., and Sultan, M. T. H., 2018. An overview of mechanical and physical testing of composite materials *Mechanical and Physical Testing of Biocomposites, Fibre-Reinforced Composites and Hybrid Composites*. Elsevier Ltd.
- Safri, S. N. A., Sultan, M. T. H., Jawaid, M., and Jayakrishna, K., 2018. Impact Behaviour of Hybrid Composites for Structural Applications: A Review. *Composites Part B: Engineering*, 133:112–121.
- Sakthivel, R., and Rajendran, D., 2014. Experimental Investigation and Analysis a Mechanical Properties of Hybrid Polymer Composite Plates. *International Journal of Engineering Trends and Technology*, 9(8):407–414.
- Scalici, T., Pitarresi, G., Badagliacco, D., Fiore, V., and Valenza, A., 2016. Mechanical Properties of Basalt Fiber Reinforced Composites Manufactured with Different Vacuum Assisted Impregnation Techniques. *Composites Part B: Engineering*, 104:35–43.
- Serin, H., Derici, O. B., and Yildizhan, S., 2019. A Review on Open Mold Techniques for Polymer Matrix Composite Products. 4th International Mediterranean Science and Engineering Congress (IMSEC 2019), Turkey
- Sezgin, H., 2018. Investigation and Enhancement of The Mechanical Properties of The Fabric Reinforced Hybrid Composites. PhD Thesis, Istanbul Technical University.
- Shahzad, A., 2009. Impact and Fatigue Properties of Natural Fibre Composites. PhD Thesis, University of Wales.

- Sureshkumar, M., Tamilselvam, P., Kumaravelan, R., and Dharmalingam, R., 2014. Design, Fabrication, and Analysis of a Hybrid FIBER Composite Monoleaf Spring Using Carbon and E-Glass Fibers for Automotive Suspension Applications. *Mechanics of Composite Materials*, 50(1): 115-122.
- Tajuddin, M., Ahmad, Z., and Ismail, H., 2016. A Review of Natural Fibers and Processing Operations for the Production of Binderless Boards. *BioResources*, 11(2):5600–5617.
- Thippesh, L., 2018. Fabrication of Hybrid Composite Mono-Leaf Spring with Unidirectional Glass Fibers. *Materials Today-Proceedings*, 5(1): 2980-2984.
- Uzay, Ç., Acer, D., and Geren, N., 2019. Impact Strength of Interply and Intraply Hybrid Laminates Based on Carbon-Aramid/Epoxy Composites. *European Mechanical Science*, 3(1):1–5.
- Xueyuan, L., 2015. Radiation Curing of Natural Fiber Composite. State University of New York College.

CURRICULUM VITAE

Okan elik, graduated from Fazilet Kibritođlu Primary School in 2007 and graduated from Ramazan Atıl Anatolian High School in 2011. Then, he started his BSc degree in 2012 at ukurova University, Automotive Engineering Department. He started his MSc education in the same department of ukurova University in 2019. He has been working as a Research Assistant in Dokuz Eylöl University, Mechanical Engineering Department.

